Turing Instabilities and Spatial Pattern Formation in One-Dimension

A Thesis
Presented to
the Faculty of the Department of Mathematical Sciences
George Mason University

In Partial Fulfillment
of the Requirements for the Degree
Bachelor of Science
Mathematics

by

Robert Francis Allen

August 2003

Turing Instabilities and Spatial Pattern Formation in One-Dimension

This thesis is submitted in partial fulfillment of the requirements for the degree of
Bachelor of Science
Mathematics

Committee Approval:

_____

Evelyn Sander (Advisor)

_____   _____

Harbir Lamba   Jeng-Eng Lin

August 2003

Acknowledgments

I can not thank my advisor, Dr. Evelyn Sander, enough for all that she has done for me. First, she was willing to be my advisor, knowing of the difficulties in me being a unique student. Secondly, she pulled me through the times when I wanted to quit. She also never gave up on me when external pressures led me away from completing my thesis. She always remained a force to get me back on track.

A special thanks goes out to my committee members, Dr. Jeng-Eng Lin and Dr. Harbir Lamba. I appreciate the time you've invested in me and my thesis. Special thanks also go out to Dr. Thomas Wanner. You were always there to help me think through issues or find sources that had exactly the information I needed.

I am also truly thankful to the Mathematics Department at George Mason University. All of my current and future success as a mathematician will be a direct reflection of you. Specifically, thank you to Dr. Flavia Colonna, Dr. David Singman, Dr. Rebecca Goldin, Dr. Jay Shapiro, Dr. Kathleen Alligood, Dr. Klaus Fischer, Dr. Robert Sachs, Ms. Ellen O'Brien, Ms. Ann Morley and Ms. Christine Amaya.

I could not have gotten through the past two years without some very special friends. Many thanks go out to Carl, Alex, DeVon, Catherine, Meredith, Jennifer, Lars, Ian, Keith & Amber and Jeff. Without you, I'm sure I would have either quit, or ended up in psychiatric care. I am a better person for knowing each and every one of you.

As with everything in my life, I could not have done it without the love and support from my family. I would not be following my dreams had it not been for them.

All animal photographs used in this thesis were take by Tony Northrup, and can be found at http://www.northrup.org

Abstract

One particular theory in Biology is that the formation of mammalian animal coat patterns is due to concentrations of activator and inhibitor chemicals called morphogens. These morphogens react and diffuse within the cell clusters; concentrations of the morphogens are the key to the spatial patterns formed in the animal coat.

The purpose of this thesis is twofold. The first purpose is to study a particular Reaction-Diffusion equation to see when it exhibits instability in its homogeneous equilibrium. These instabilities, known as Turing instabilities, are where the animal coat patterns form. The second purpose is the determine via Numerical Methods the stability of the solutions of the Reaction-Diffusion equation near these Turing instabilities. These solutions are the key as to the actual patterns that form. We will compare the stability of these solutions to published data by Murray.

I do not know what I may appear to the world; but to myself I seem to have been only like a boy, playing on the sea-shore, and diverting myself, in now and then finding a smoother pebble, or a prettier shell than ordinary, whilst the great ocean of truth lay all undiscovered before me.

— Sir Isaac Newton

Contents

Figures

Tables

Listings

Chapter 1

Background

1.1 Motivation

The development of animal coat patterns in mammals has been an area of study by biologists. A theory of how these patterns occur was introduced by a mathematician, Alan Turing [13]. Turing introduced a model by which spacial patterns can grow in a particular type of equation from a homogeneous equilibrium under certain circumstances. We will discuss the model by which these patterns form mathematically.

1.1.1 Natural Motivation

Morphogenesis is the biological process by which form and structure is created during embryonic development. Once the egg is fertilized, it begins to divide. At a certain period during gestation, the cells begin to differentiate (biologically speaking). Cell differentiation is based on location within the group of cells [9]. This process is not enough, however, to determine how the spots are formed on a leopard, or the stripes on a zebra.

The notion of how animal coat patterns are formed is a process that occurs well after cell division and differentiation. The color of hair in animal coats is due to pigment cells called melanocytes. These cells are found in the innermost layer of the skin. The melanocytes create pigment, known as melanin, which passes into and thus colors the hair. There are essentially only two types of melanin, one that produces black and brown hair color, and one that produces yellow and red hair color.

Some Biologists believe that melanocytes produce melanin based on the presence of certain activator and inhibitor chemicals [9]. Each animal coat pattern is thought to be the product of some chemical pattern of these activators and inhibitors [8].

1.1.2 Mathematical Motivation

In 1952, the mathematician Alan Turing published a paper in Theoretical Biology on the Chemical Basis of Morphogenesis [13]. This paper put forth a model for spatial pattern formation which is studied to this day. The model states that a set of chemicals reacting and diffusing throughout tissue may exhibit spatial patterns under the proper circumstances. The model is that of a system of partial differential equations aptly named a Reaction-Diffusion Model. The condition is that the equilibrium solution, in the absence of diffusion, be linearly stable and unstable in the presence of diffusion. Much study has been conducted as to the particulars of patterns formed [9], and the mechanisms by which the patterns are selected in higher dimensions [12].

Spatial instabilities close to this homogeneous equilibrium produce patterns in the concentrations of the chemicals in the system. These patterns can be thought of as the key to the actual patterns of an animal coat, such as zebra stripes or leopard spots. These spatial instabilities are known as Turing instabilities, or diffusion-driven instabilities. These patterns are the subject of this thesis.

1.2 Reaction-Diffusion Model

A model under considerable study to explain the formation of mammalian coat patterns is the Reaction-Diffusion Model. In this model, a set of objects are able to react with each other, and move, or diffuse, through the domain. Applied to animal coat patterns, a system of two morphogens are modelled by the following system of equations on a domain $\Omega \subset \mathbb{R}^n$

$$
\begin{aligned}
u_t &= \quad \Delta u + \gamma \cdot f(u,v) \\
v_t &= d\Delta v + \gamma \cdot g(u,v),
\end{aligned}
\tag{1.1}
$$

where $u(\mathbf{x},t), v(\mathbf{x},t) : \Omega \to \mathbb{R}$ represent the concentrations of the two morphogens, with f and g, the reaction kinetics of u and v respectively. This system of partial differential equations is modelled as an isolated system, meaning no external influences are present. To formalize this notion, homogeneous Neumann boundary conditions [11] are applied to the model, namely

$$
\begin{aligned}
(\nabla u \cdot \mathbf{n})(\mathbf{x}) &= 0 \\
(\nabla v \cdot \mathbf{n})(\mathbf{x}) &= 0,
\end{aligned}
\tag{1.2}
$$

$\forall x \in \partial\Omega$ and $\mathbf{n}$ the unit outward normal of $\partial\Omega$.

1.2.1 Applicability to Situation

The reaction kinetics that we will study are those described by equation (1.3). This set of non-linearities was proposed by Thomas and thus will be referred to as the Thomas system. Much research has been done with various reaction kinetics. Murray [9] provides much data using the Thomas system with constants (1.4). We will use this non-linear system for comparison with published data.

$$
\begin{aligned}
f(u,v) &= a - u - h(u,v) \\
g(u,v) &= \alpha(b - v) - h(u,v) \\
h(u,v) &= \frac{\rho \cdot u \cdot v}{1 + u + Ku^2}
\end{aligned}
\tag{1.3}
$$

$$
a = 150, \ b = 100, \ \alpha = 1.5, \ \rho = 13, \ \text{and } K = 0.05.
\tag{1.4}
$$

1.2.2 Derivation

In deriving the reaction-diffusion system (1.1), we will employ a continuum approach, as in [6]. There are many other approaches to deriving the model, including combinatoric and probabilistic methods ([6] and [9]).

Let $\mathbf{c}(\mathbf{x},t) : \Omega \times \mathbb{R}^n \to \mathbb{R}$ be the concentration of morphogens in the system. Let $\mathbf{Q}(\mathbf{x},t)$ be the net creation rate of morphogens at $\mathbf{x} \in \Omega$ at time t. Let $\mathbf{J}(\mathbf{x},t)$ be the flux density. For any unit vector $\mathbf{n} \in \mathbb{R}^n$, $\mathbf{J} \cdot \mathbf{n}$ is the net rate at which morphogens cross a unit area in a plane perpendicular to $\mathbf{n}$. For our purposes, we will assume $\mathbf{J}$ to be smooth, that is $\mathbf{J} \in C^1$.

Let $B \subset \Omega$ be closed and integrable. We denote the morphogen mass in B by

$$
\int_B c \, dV,
$$

where $dV = dx_1 \cdots dx_n$ for $\mathbf{x} = (x_1, \ldots, x_n)^T$. If we assume the rate of change of the morphogen mass is due to particle creation and degradation in B and flow though ∂B, then

$$
\frac{d}{dt} \int_B c \, dV = \int_{\partial B} \mathbf{J} \cdot \mathbf{n} \, dA + \int_B \mathbf{Q} \, dV.
$$

Differentiating through the left hand side, and applying the Divergence Theorem to the right hand side, we obtain

$$
\int_b c_t \, dV = \int_B (-\nabla \cdot \mathbf{J} + \mathbf{Q}) \, dV.
$$

Since B is an arbitrary subset of the domain, it must hold that

$$
c_t = -\nabla \cdot \mathbf{J} + \mathbf{Q}.
\tag{1.5}
$$

Equation (1.5) represents a conservation law.

For the model, we must specify both **J** and **Q**. For the flux density we will apply Fick's Law [6]. Thus

$$\mathbf{J} = -D\nabla\mathbf{c}.$$

$D \in M_n(\mathbb{R})$ is has positive entries and is called the diffusivity. Applying Fick's Law to (1.5) results in

$$\mathbf{c}_t = D\Delta\mathbf{c} + \mathbf{Q}.$$

Q is the reaction kinetics, and thus for our system, is a function of the concentration levels of the morphogens; **Q** is a function of **c**. Thus, the general form for the reaction diffusion model is

$$\mathbf{c}_t = D\Delta\mathbf{c} + \mathbf{Q}(\mathbf{c}). \tag{1.6}$$

The specific model we will be studying is a two morphogen system. Thus we have

$$\mathbf{c}(\mathbf{x},t) = \begin{pmatrix} u(\mathbf{x},t) \\ v(\mathbf{x},t) \end{pmatrix}, \tag{1.7}$$

$$D = \begin{pmatrix} 1 & 0 \\ 0 & d \end{pmatrix}, \tag{1.8}$$

and

$$\mathbf{Q}(u,v) = \gamma \begin{pmatrix} f(u,v) \\ g(u,v) \end{pmatrix}. \tag{1.9}$$

By applying (1.7), (1.8) and (1.9) to (1.6), we obtain (1.1).

1.2.3   Equilibrium Solution

One type of solution of particular interest is the equilibrium solution of a partial differential equation. Specifically of interest are attracting equilibrium solutions. These are time-independent solutions which are stable to small perturbations. Stability comes in many forms. We wish to classify equilibria which are linearly stable.

Equilibrium solutions to (1.1) are solutions $(u_0, v_0)^T$ such that $u_t = v_t = 0$. Thus, (1.1) turns into

$$\begin{aligned} 0 &= \quad \Delta u + \gamma \cdot f(u,v) \\ 0 &= \quad d\Delta v + \gamma \cdot g(u,v). \end{aligned} \tag{1.10}$$

For the modelling of animal coat patterns, equilibria in the absence of diffusion are of key

importance. A system without diffusion would have $\Delta u = \Delta v = 0$. Thus, (1.10) becomes

$$
\begin{aligned}
0 &= f(u,v) \\
0 &= g(u,v).
\end{aligned}
\tag{1.11}
$$

So, for our model, equilibrium solutions in the absence of diffusion are those solutions $(u_0, v_0)^T$ which solve $f(u_0, v_0) = g(u_0, v_0) = 0$. Note that the definition of the reaction kinetics in (1.3) is not dependent on γ or d. Thus, the equilibrium solution is independent of these parameters.

Since (1.10) is a non-linear system, we must employ numerical methods to solve the roots of this system. Newton's Method for systems of non-linear systems [7] was used to solve this system. The equilibrium solution is calculated to be

$$
\begin{pmatrix} u_0 \\ v_0 \end{pmatrix} = \begin{pmatrix} 37.73821081921373 \\ 25.15880721280914 \end{pmatrix}.
\tag{1.12}
$$

Now, the question of stability of the equilibrium solutions is addressed. An equilibrium solutions is linearly stable if its linearization attracts small perturbations. We define a perturbation of the equilibrium solution as

$$
\mathbf{w} = \begin{pmatrix} u - u_0 \\ v - v_0 \end{pmatrix}.
$$

Equation (1.3) can be linearized about (u_0, v_0) by the following

$$
\begin{aligned}
f(u,v) &\approx \left[\overset{=0}{\overbrace{f(u_0, v_0)}} \right] + f_u(u_0, v_0) \cdot (u - u_0) + f_v(u_0, v_0) \cdot (v - v_0) \\
&= f_u(u_0, v_0) \cdot (u - u_0) + f_v(u_0, v_0) \cdot (v - v_0),
\end{aligned}
$$

and similarly,

$$
\begin{aligned}
g(u,v) &\approx \left[\overset{=0}{\overbrace{g(u_0, v_0)}} \right] + g_u(u_0, v_0) \cdot (u - u_0) + g_v(u_0, v_0) \cdot (v - v_0) \\
&= g_u(u_0, v_0) \cdot (u - u_0) + g_v(u_0, v_0) \cdot (v - v_0),
\end{aligned}
$$

If we remove diffusion from (1.1) we obtain

$$
\begin{aligned}
u_t &= \gamma \cdot f(u,v) \\
v_t &= \gamma \cdot g(u,v).
\end{aligned}
\tag{1.13}
$$

Linearizing (1.13) about (u_0, v_0), we obtain the following system

$$u_t = \gamma \cdot [f_u(u_0, v_0) \cdot (u - u_0) + f_v(u_0, v_0) \cdot (v - v_0)]$$
$$v_t = \gamma \cdot [g_u(u_0, v_0) \cdot (u - u_0) + g_v(u_0, v_0) \cdot (v - v_0)]$$

which can be written in matrix form

$$\mathbf{w}_t = \gamma \cdot A \cdot \mathbf{w}, \ A = \begin{pmatrix} f_u(u_0, v_0) & f_v(u_0, v_0) \\ g_u(u_0, v_0) & g_v(u_0, v_0) \end{pmatrix}. \tag{1.14}$$

In linearizing (1.13), we have reduced the partial differential equation into a linear ordinary differential equation. The solution $\mathbf{w}$ is said to be linearly stable if $|\mathbf{w}| \to 0$ as $t \to \infty$. We wish to determine the conditions on the eigenvalues of $\gamma \cdot A$ which make the solution $\mathbf{w}$ linearly stable. The proof of the following theorem is an adaptation of a proof from [10].

Theorem 1.1. *The solution, $\mathbf{w}$, of equation (1.14) is linearly stable if and only if all eigenvalues of $\gamma \cdot A$ have negative real part.*

Proof. Given an initial perturbation, $\mathbf{w}(0) = \mathbf{w}_o$, the Fundamental Theorem for Linear Systems [10] states that there exists a unique solution given by $\mathbf{w}(t) = e^{\gamma A t} \mathbf{w}_0$. Thus, $\mathbf{w}(t)$ is linearly stable if and only if

$$\lim_{t \to \infty} \mathbf{w} = \lim_{t \to \infty} e^{\gamma A t} \mathbf{w}_0 = 0.$$

($\Rightarrow$) Assume one eigenvalue of γA, $\lambda = a + ib$ has positive real part ($a > 0$). Then by [10], there exists $\mathbf{w}_0 \in \mathbb{R}^2$ such that $\mathbf{w}_0 \neq 0$ and $\left| e^{\gamma A t} \mathbf{w}_0 \right| \geq e^{at} |\mathbf{w}_0|$. Clearly $\left| e^{\gamma A t} \mathbf{w}_0 \right| \to \infty$ as $t \to 0$, and thus

$$\lim_{t \to \infty} e^{\gamma A t} \mathbf{w}_0 \neq 0.$$

Assume one eigenvalue of γA, $\lambda = ib$, has zero real part. Then by [10], there exists $\mathbf{w}_0 \in \mathbb{R}^2$ such that $\mathbf{w}_0 \neq 0$ and one component of the solution is of the form $ct^k \cos bt$ or $ct^k \sin bt$ for $k \geq 0$. Again,

$$\lim_{t \to \infty} e^{\gamma A t} \mathbf{w}_0 \neq 0.$$

Thus, if any eigenvalue has real part greater than or equal to zero, we can not have a stable solution. We will now show that if the real part of the eigenvalue is negative, we obtain stability.

($\Leftarrow$) If all eigenvalues of γA have negative real part, then by [10], there exist positive constants a, m, M_1 and $k \geq 0$ such that

$$m|t|^k e^{-at} |\mathbf{w}_0| \leq |e^{\gamma A t} \mathbf{w}_o| \leq M_1 (1 + |t|^k) e^{-ct} |\mathbf{w}_0|$$

for all $\mathbf{w_0} \in \mathbb{R}^2$ and $t \in \mathbb{R}$. We see that $(1 + |t|^k) e^{-(a-c)t}$ is bounded when $0 < c < a$. Thus we have

when $0 < c < a$, there exists $M > 0$ such that

$$m|t|^k e^{-at}|\mathbf{w}_0| \le |e^{\gamma At}\mathbf{w}_o| \le M e^{-ct}|\mathbf{w}_0| \tag{1.15}$$

for all $\mathbf{w}_0 \in \mathbb{R}^2$ and $t \in \mathbb{R}$.

If we take the limit as $t \to \infty$ to both sides of inequality (1.15), we see by the Squeeze Theorem that

$$\lim_{t \to \infty} \left| e^{\gamma At}\mathbf{w}_0 \right| = 0.$$

■

1.2.4 Diffusion Equation

Now we will consider solutions (1.1) in the absence of reactions, purely diffusion. With no reaction kinetics, $f(u,v) = g(u,v) = 0$, and thus we have

$$\begin{aligned} u_t &= \Delta u \\ v_t &= d\Delta v. \end{aligned} \tag{1.16}$$

Let $\mathbf{w} = (u,v)^T$. We can rewrite (1.16) in the matrix form

$$\mathbf{w}_t = D\Delta\mathbf{w} \text{ , where } D = \begin{pmatrix} 1 & 0 \\ 0 & d \end{pmatrix}. \tag{1.17}$$

Equation (1.17) is sometimes called the Heat equation or the Diffusion equation. It is a model for the physical process of heat flow or diffusion through a body.

To solve this equation, we must prescribe both boundary and initial conditions. Homogeneous Neumann boundary conditions on $\Omega = [0,1]$ will be used, thus

$$\mathbf{w}_x(0) = \mathbf{w}_x(1) = 0$$

The initial conditions will be specified generically;

$$\mathbf{w}(\mathbf{x},0) = \begin{pmatrix} \Psi_0(\mathbf{x}) \\ \Phi_0(\mathbf{x}) \end{pmatrix}.$$

The equilibrium solutions previously solved were independent of domain. The solutions to the Diffusion equation are, however, not so simple. Thus, it is important to note again that the domain under which our system is modelled is $\Omega = [0,1] \subset \mathbb{R}$.

The method of Separation of Variables will be used to solve the 1-dimensional diffusion equation with homogeneous boundary conditions. First, we assume the solution to (1.17) can be written

as the product of two functions, one time-dependent, and the other space-dependent. Formally, this is stated as

$$\mathbf{w}(x,t) = \varphi(x)s(t) \tag{1.18}$$

with $\varphi(x) \not\equiv 0$ and $s(t) \not\equiv 0$. Substituting this into (1.17) we obtain

$$\varphi(x)s'(t) = s(t)\varphi_{xx}(x). \tag{1.19}$$

We can now write (1.19) as

$$\frac{s'}{s} = \frac{\varphi_{xx}}{\varphi}.$$

Since φ_{xx}/φ is independent of time, and s'/s is independent of space, then each must be independent of both, thus we can write

$$\frac{s'}{s} = \frac{\varphi_{xx}}{\varphi} = -k$$

for some $k \in \mathbb{R}$.

Thus, we have reduced the second order partial differential equation to a system to the two ordinary differential equations

$$\begin{aligned} s' &= -ks \\ -\varphi_{xx} &= k\varphi. \end{aligned} \tag{1.20}$$

1.2.4.1 Time Dependent Solution

The first step in solving the Diffusion equation is to solve the time dependent part, namely $s(t)$. We wish to write down the general solution to

$$\frac{ds}{dt} = -ks. \tag{1.21}$$

Equation (1.21) is a first order linear homogeneous differential equation with constant coefficients. It has characteristic polynomial $r = -k^2$, which has one real root. Thus by [2], the general solution to (1.21) is

$$s(t) = ce^{-kt}. \tag{1.22}$$

It is important to note that at this point the constant k is arbitrary, with no restrictions. However, the solution to the spatial equation will restrict the values of which k can take. If $k < 0$, then the solution exponentially increases as $t \to \infty$. The physical reality prevents this case from happening, as we will see in the next section.

1.2.4.2   Spatial Solution (Eigenvalue Problem)

The second equation to solve for the separation of variables method is the spatial dependent solution,

$$-\Delta\varphi = k\varphi \tag{1.23}$$

under homogeneous Neumann boundary conditions. Solutions to equation (1.23) can be considered eigenfunctions of the operator $-\Delta$ with eigenvalue k. Thus, we refer to equation (1.23) as an eigenvalue problem.

Since our domain is $\Omega = [0,1] \subset \mathbb{R}$, we can rewrite equation (1.23) as

$$-\varphi_{xx} = k\varphi, \tag{1.24}$$

which is a second order linear homogeneous ODE with constant coefficients. The characteristic polynomial for equation (1.24) is $-r^2 = k$ which has roots $\pm\sqrt{-k}$.

If $k > 0$, then the roots to the characteristic polynomial are purely imaginary, $r = \pm i\sqrt{k}$. By [2], the general solution to equation (1.24) is

$$\varphi(x) = c_1 \cos(\sqrt{k}x) + c_2 \sin(\sqrt{k}x). \tag{1.25}$$

The boundary conditions can be written as $\varphi'(0) = \varphi(1) = 0$. We can see that by applying the boundary condition at $x = 0$, we obtain

$$\varphi'(x) = -c_1\sqrt{k}\sin(\sqrt{k}x) + c_2\sqrt{k}\cos(\sqrt{k}x)$$
$$\varphi'(0) = c_2\sqrt{k} = 0$$
$$\Rightarrow c_2 = 0 \text{ since } k > 0.$$

The general solution can now be simplified to $\varphi(x) = c_1\cos(\sqrt{k}x)$. By next applying the boundary condition at $x = 1$ we will see that we get a restriction on the values k may obtain.

$$\varphi'(1) = -c_1\sqrt{k}\sin(\sqrt{k}) = 0$$
$$\Rightarrow \sqrt{k} = n\pi, n \in \mathbb{Z} \setminus \{0\}$$
$$\Rightarrow k = n^2\pi^2.$$

We do not consider the case of $c_1 = 0$, since this would result in an eigenfunction $\varphi \equiv 0$, which can not be an eigenfunction by definition. Thus, for $k > 0$ we have eigenfunctions $\varphi_k(x) = c_1\cos(\sqrt{k}x) = c_1\cos(n\pi x)$ with eigenvalue $k = n^2\pi^2$.

If $k = 0$, the characteristic polynomial of equation (1.23) is $r^2 = 0$ with repeated real root $r = 0$. Thus the general solution of equation (1.23) is $\varphi(x) = c_1 + c_2x$. Under the boundary conditions, we

have $\varphi'(0) = \varphi'(1) = c_2 = 0$. Thus the general form of the solution is simply $\varphi(x) = c_1$.

If $k < 0$, then we want to solve the second order linear homogeneous ODE

$$\varphi_{xx} = k^*\varphi$$

where $k^* = -k > 0$. The characteristic polynomial for this ODE is $r^2 = k^*$ which has two real roots $r = \pm\sqrt{k^*}$. The general solution to this equation is $\varphi(x) = c_1 e^{\sqrt{k^*}x} + c_2 e^{-\sqrt{k^*}x}$. If we apply the boundary condition at $x = 1$, we see a problem with this solution. $\varphi'(x) = c_1\sqrt{k^*}e^{\sqrt{k^*}x} - c_2\sqrt{k^*}e^{-\sqrt{k^*}x} = 0$ implies that $c_1 = c_2 = 0$, since $e^{\sqrt{k^*}x} \neq 0$ and $e^{-\sqrt{k^*}x} \neq 0 \forall x \in \Omega$. Thus, for $k < 0$ we only obtain trivial solutions to the eigenvalue problem. Thus, we will note that $k \nleq 0$.

So, we have the eigenvalues and eigenfunctions of the $-\Delta$ operator under homogeneous Neumann boundary conditions are

$$k = n^2\pi^2, n \in \mathbb{Z}$$
$$\varphi_k(x) = c_1\cos(\sqrt{k}x) = c_1\cos(n\pi x). \tag{1.26}$$

It is important to note that for $n \in \mathbb{Z}$, $n^2\pi^2 \geq 0$, and thus $k \geq 0$.

1.2.4.3 General Solution to the Diffusion Equation

Equation (1.18) describes the solution to the Diffusion equation as the product of two functions, one time dependent and one space dependent. As described in the previous two sections, the general form of the solution for the Diffusion equation is

$$\begin{aligned}\mathbf{w}(x,t) &= \sum_{n=0}^{\infty} c_n\varphi_n(x)s_n(t) \\ &= \sum_{n=0}^{\infty} c_n e^{-n^2\pi^2 t}\cos(n\pi x)\end{aligned} \tag{1.27}$$

where the coefficient terms c_n are determined from the Fourier expansion of the initial conditions

$$\mathbf{w}_0 = \sum_{n=0}^{\infty} c_n\cos(n\pi x).$$

The method of separation of variables is not guaranteed to find all solutions to the Diffusion equation in general. However, for the one-dimensional Diffusion equation with homogeneous Neumann boundary conditions, separation of variables gives all solutions [3]. Thus, equation (1.27) fully describe the solutions to the Diffusion equation.

1.3   Turing Instability

Patterns are formed through the instability of the homogeneous steady-state solution to small spatial perturbations. If the homogeneous steady-state solution was stable, then small perturbations from the steady-state would converge back to the steady-state. Alan Turing, in [13], showed how a Reaction-Diffusion system can exhibit such instabilities to form patterns. We will present the conditions under which Turing instabilities can occur (as described in [9]), and show that the Thomas system meets these conditions, and thus will exhibit Turing instabilities.

1.3.1   Existence of Turing Instabilities

This section will present a derivation of the necessary and sufficient conditions for Turing instabilities to be present in a Reaction-Diffusion model, as presented in [9]. For completeness, we will define the Reaction-Diffusion model as

$$\mathbf{w}_t = D\Delta\mathbf{w} + \gamma\cdot\mathbf{F}(\mathbf{w}) \tag{1.28}$$

with

$$\mathbf{w} = \begin{pmatrix} u(x,t) \\ v(x,t) \end{pmatrix}, \ D = \begin{pmatrix} 1 & 0 \\ 0 & d \end{pmatrix}, \ \mathbf{F}(\mathbf{w}) = \begin{pmatrix} f(\mathbf{w}) \\ g(\mathbf{w}) \end{pmatrix}$$

and $d,\gamma > 0$ on the domain $\Omega = [0,1]$ with initial conditions $u(\mathbf{x},0)$ and $v(\mathbf{x},0)$, and Neumann boundary conditions. If Neumann boundary conditions are not chosen, then the solutions to equation (1.28) will be partially determined by the boundary conditions. We choose to model an isolated system with no external influences, hence the choice of Neumann boundary conditions.

The first condition under which Turing instabilities form is a condition imposed on the steady-state solution in the absence of diffusion. For diffusion-driven instability to occur, the homogeneous steady-state solution must be linearly stable in the absence of any spatial variation [9]. In Theorem 1.1, we proved the linear stability of the homogeneous steady-state solution (u_0, v_0) to be exactly when $\mathrm{Re}\,\lambda_1 < 0$ and $\mathrm{Re}\,\lambda_2 < 0$ for λ_1 and λ_2 being the eigenvalues of the stability matrix

$$\gamma A = \gamma \begin{pmatrix} f_u(u_0, v_0) & f_v(u_0, v_0) \\ g_u(u_0, v_0) & g_v(u_0, v_0) \end{pmatrix} = \gamma \begin{pmatrix} f_u & f_v \\ g_u & g_v \end{pmatrix}_{u_0, v_0}.$$

To calculate the eigenvalues of A, we simply solve

$$|\gamma A - \lambda I| = \left| \begin{pmatrix} \gamma f_u - \lambda & \gamma f_v \\ \gamma g_u & \gamma g_v - \lambda \end{pmatrix} \right| = 0$$

$$\Rightarrow (\gamma f_u - \lambda)(\gamma g_v - \lambda) - \gamma^2 f_v g_u = 0$$

$$\Rightarrow \lambda^2 - \gamma(f_u + g_v) + \gamma^2(f_u g_v - f_v g_u) = 0$$

$$\Rightarrow \lambda_1, \lambda_2 = \gamma \frac{(f_u + g_v) \pm \sqrt{(f_u + g_v)^2 - 4(f_u g_v - f_v g_u)}}{2}$$

Linear stability is guaranteed if

$$\operatorname{tr} A = f_u + g_v < 0$$
$$|A| = f_u g_v - f_v g_u > 0. \tag{1.29}$$

We will now consider the full Reaction-Diffusion equation. Linearizing equation (1.28) about the steady-state (u_0, v_0) in the same manner as done to derive equation (1.14) we get

$$\mathbf{w}_t = \gamma A \mathbf{w} + D \Delta \mathbf{w}, \; A = \begin{pmatrix} f_u & f_v \\ g_u & g_v \end{pmatrix}_{u_0, v_0}, \; D = \begin{pmatrix} 1 & 0 \\ 0 & d \end{pmatrix}. \tag{1.30}$$

Substituting (1.27) into (1.30) results in

$$w_t = \gamma A w + D \Delta w$$

$$\sum_{n=0}^{\infty} c_n \lambda_n e^{-\lambda_n t} \cos(n\pi x) = \sum_{n=0}^{\infty} \gamma A c_n e^{-\lambda_n t} \cos(n\pi x) + \sum_{n=0}^{\infty} -D c_n e^{-\lambda_n t} n^2 \pi^2 \cos(n\pi x).$$

For each $n \in \mathbb{Z}$, we have

$$c_n \lambda_n e^{\lambda_n t} \cos(n\pi x) = \gamma A c_n e^{-\lambda_n t} \cos(n\pi x) - D c_n e^{-\lambda_n t} n^2 \pi^2 \cos(n\pi x)$$

$$\lambda_n \cos(n\pi x) = \gamma A \cos(n\pi x) - D n^2 \pi^2 \cos(n\pi x)$$

$$\lambda_n \varphi_n(x) = \gamma A \varphi_n(x) - D k^2 \varphi_n(x)$$

$$0 = (\lambda_n - \gamma A + D k^2) \varphi_n(x).$$

Since $\varphi_n(x)$ is non-trivial $\forall n$ by construction, we must have that $|\lambda_n I - \gamma A + k^2 D| = 0$. For conve-

nience we will drop the subscript on λ. Thus,

$$\left|\lambda I - \gamma A + k^2 D\right| = 0$$

$$\left|\begin{pmatrix} \lambda - \gamma f_u + k^2 & -\gamma f_v \\ -\gamma g_u & \lambda - \gamma g_v + k^2 d \end{pmatrix}\right| = 0$$

$$\Rightarrow (\lambda - \gamma f_u + k^2)(\lambda - \gamma g_v + k^2 d) - (-\gamma f_v)(-\gamma g_u) = 0$$

$$\Rightarrow \lambda^2 + \lambda \left[k^2(1+d) - \gamma(\operatorname{tr} A)\right] + h(k^2) = 0,$$

where $h(k^2) = dk^4 - \gamma(df_u + g_v)k^2 + \gamma^2 |A|$.

We have already imposed restrictions (1.29) to the steady-state solution in the absence of diffusion, which must be applied to the general solution as well. Consider the conditions under which the steady-state solution is unstable to with respect to perturbations, namely Re $\lambda > 0$ for some $k \neq 0$. This instability with respect to spatial perturbations is exactly what is needed for the formation of patterns. Without this instability, small spatial perturbations would converge to the homogeneous steady-state solution.

This can occur if the coefficient of λ is negative, or if $h(k^2) < 0$. However, by (1.29), $\operatorname{tr} A < 0$, and since $d > 0$, $k^2(1+d) > 0$. So,

$$k^2(1+d) - \gamma(\operatorname{tr} A) > 0.$$

So, the only possibility for Re $\lambda > 0$ comes when $h(k^2) < 0$.

The only possibility for $h(k^2) < 0$ is if $|A| < 0$ or $df_u + g_v > 0$. But by (1.29), $|A| > 0$, so the only condition is if $df_u + g_v > 0$. We can see clearly that $d \neq 1$, since if it did, then $f_u + g_v > 0$ which contradicts (1.29). Thus, a third criterion for Turing instabilities is

$$df_u + g_v > 0. \tag{1.31}$$

Criterion (1.31) is sufficient, but not necessary, for Re $\lambda > 0$. For $h(k^2)$ to be negative for some $k > 0$, the minimum must be negative. With a change of variables, $z = k^2$, and simple calculus, we can calculate the minimum of $h(k^2)$ as follows

$$h(z) = dz^2 - \gamma(df_u + g_v)z + \gamma^2 |A|$$

$$\frac{dh}{dz} = 2dz - \gamma(df_u + g_v)$$

$$\frac{dh}{dz} = 0 \Rightarrow 2dz - \gamma(df_u + g_v) = 0$$

$$\Rightarrow z^* = \frac{\gamma(df_u + g + v)}{2d}$$

It is clear that h is concave up on it's entire domain, by the second derivative test, and thus h will attain it's minimum at z^*. Thus

$$
\begin{aligned}
h_{min} &= h(z^*) \\
&= d\left[\frac{\gamma(df_u+g_v)}{2d}\right]^2 - \gamma(df_u+g_v)\left[\frac{\gamma(df_u+g_v)}{2d}\right] - \gamma^2|A| \\
&= \frac{\gamma^2(df_u+g_v)^2}{4d} - \frac{2\gamma^2(df_u+g_v)^2}{4d} - \gamma^2|A| \\
&= \gamma^2\left[|A| - \frac{(df_u+g_v)^2}{4d}\right].
\end{aligned}
$$

Thus, the condition that $h(k^2) < 0$ for some $k \in \mathbb{N}$ is

$$
\begin{aligned}
h_{min} &< 0 \\
\gamma^2\left[|A| - \frac{(df_u+g_v)^2}{4d}\right] &< 0 \\
|A| - \frac{(df_u+g_v)^2}{4d} &< 0 \\
\frac{(df_u+g_v)^2}{4d} &> |A|.
\end{aligned}
$$

Thus, the necessary and sufficient conditions for the presence of Turing instabilities in (1.28) are

$$
\begin{aligned}
f_u + g_v &< 0 \\
f_u g_v - f_v g_u &> 0 \\
df_u + g_v &> 0 \\
(df_u + g_v)^2 - 4d(f_u g_v - f_v g_u) &> 0,
\end{aligned}
\tag{1.32}
$$

recalling that all partial derivatives are evaluated at (u_0, v_0).

1.3.2 Existence of Turing Instabilities in the Thomas System

The Reaction-Diffusion model specified by equation (1.1) is quite general, and without specifying the reaction-kinetics, would be impossible to study numerically. Thus, the work presented here focuses on the study of the Thomas System. We will now show that it is possible for the Thomas System to exhibit Turing instabilities by verifying it meets the criteria of (1.32).

From equation (1.3) we can calculate the first order partial derivatives evaluated at the homoge-

neous steady state solution (1.12) as

$$
\begin{aligned}
f_u &= 0.89958351470112 \\
f_v &= -4.46212685010084 \\
g_u &= 1.89958351470112 \\
g_v &= -5.96212685010084
\end{aligned}
\tag{1.33}
$$

We will now determine for what d the criteria of (1.32) are met. It is clear to see that $f_u + g_v = -5.06254333539971 < 0$ and $f_u g_v = f_v g_u = 3.11275157804915 > 0$, thus the first two conditions are met. For the third condition, the function $f(d) = f_u \cdot d + g_v$ is a linear increasing function (since $d > 0$) with x-intercept of $d = \frac{-g_v}{f_u} = 6.62765241099565$. Thus, for all $d > 6.62765241099565$, $d f_u + g_v > 0$.

The last condition forms a quadratic equation $f(d) = f_u^2 \cdot d^2 + (4 f_v g_u - 2 f_u g_v)d + g_v^2$. f is concave up and has roots at $d_1 = 1.31581376525321$ and $d2 = 21.86205460075870$. Thus we know that $f(d) > 0$ for all $d \in (-\infty, d_1) \bigcup (d_2, \infty)$. Since the restrictions for condition 3 to hold are $d > 6.62765241099565$, we conclude that for all four conditions to hold, $d > 21.86205460075870$. Thus, we have the conditions for which Turing instabilities occur in the Thomas system.

1.4 Purpose of Thesis

The purpose of this thesis is the develop some quantitative notion of the solution to equation (1.1) on the domain $\Omega = [0, 1] \subset \mathbb{R}$. In this first part of this thesis, the bifurcation structure of (1.1) under the reaction kinetics (1.3) will be developed. Both analytical and numerical methods will be used to develop the structure. The bifurcations from equilibrium can be developed analytically. The branches from the bifurcations are developed numerically using AUTO.

The second part of this thesis is the verification of results based on Murray [9]. In his development of the relationship of scale and geometry to the solution of the Thomas system, he provides the solutions of the system as a function of γ and d. It is my contention that this depiction is not accurate. The last part of this thesis will develop a more accurate diagram, developed through numerical methods.
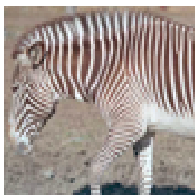
Chapter 2

Numerical Methods

Two software systems are utilized in the numerical calculations of this thesis. To calculate bifurcation branches and equilibrium solutions, we utilize AUTO. To compute time-dependent solutions and analyze stability of the calculated solutions, we utilize custom written MATLAB software termed the Stability System.[1] Solutions calculated by AUTO are used as input into the Stability System. The Stability System evolves solutions over time at fixed spatial intervals. AUTO computes solutions using adaptive methods, and provides solutions at non-fixed intervals. Clamped cubic splines are utilized to approximate the solutions calculated by AUTO at the fixed spatial intervals required by the Stability System.

2.1 Bifurcation Analysis with AUTO

AUTO [5] uses Pseudo-arclength continuation with Newton's Method as a Predictor-Corrector scheme to trace solution branches bifurcating off of the homogeneous equilibrium [4], described in the following section. AUTO is also used to compute equilibrium solutions for the Thomas system. These solutions are input for the Stability software, described in the following section.

2.1.1 Thomas System for AUTO

AUTO can do limited bifurcation analysis of systems of ordinary differential equations of the form

$$u'(t) = f(u(t), p), \;\; f(\cdot, \cdot), u(\cdot) \in \mathbb{R}^n, \tag{2.1}$$

where p denotes one or more free parameters [5]. Since we want to have AUTO calculate bifurcations along the equilibrium of the Thomas system, we must rewrite equation (1.10) to be of the form of equation (2.1).

---

[1]The code used for the time-dependent simulations was developed by Sander and Wanner for [12].

To rewrite a system of second order ODEs as a system of first order ODEs, we employ a standard trick of introducing new equations to the system. We will utilize the following equations

$$w(x) = u'(x)$$
$$z(x) = v'(x)$$

(2.2)

and thus can write equation (1.10) as

$$u'(x) = w(x)$$
$$w'(x) = -\gamma \cdot f(u, v)$$
$$v'(x) = z(x)$$
$$z'(x) = -\frac{\gamma \cdot g(u, v)}{d}.$$

(2.3)

2.1.2 Arclength Continuation

Equation (2.3) contains two system parameters, γ and d. For the computations of this thesis, we will fix d and vary γ, referred to as the continuation parameter. We can write equation (2.3) as

$$\dot{\omega} = F(\omega, \gamma), \ \ \gamma \in \mathbb{R}, \ \omega = (w, u, z, v)^T.$$

To calculate the equilibrium solutions to equation (2.3), we need to solve the non-linear system

$$0 = F(\omega, \gamma).$$

(2.4)

AUTO uses Predictor-Corrector continuation to solve equation (2.4), specifically Pseudo-arclength continuation (predictor) with Newton's method (corrector). The use of Predictor-Corrector continuation instead of relying on some simple numerical method, such as Newton's method alone, is the difficulty Newton's method has with turning points. Solution branches can fold and turn in ways that would make Newton's method diverge.

We parameterize equation (2.4) by arclength s. Thus, $(\omega, \gamma) = \left((w(s), u(s), z(s), v(s))^T, \gamma(s)\right)$ and

$$\left(\frac{dw}{ds}\right)^2 + \left(\frac{du}{ds}\right)^2 + \left(\frac{dz}{ds}\right)^2 + \left(\frac{dv}{ds}\right)^2 + \left(\frac{d\gamma}{ds}\right)^2 = 1.$$

(2.5)

Given a solutions along the solution branch, $(\omega(s_i), \gamma(s_i))$, we predict the next solution $(\omega(s_{i+1}), \gamma(s_{i+1}))$ along the tangential vector at (ω_i, γ_i) of fixed length Δs.

We can approximate equation (2.5) by

$$
\begin{aligned}
1 &= \left(\frac{dw}{ds}\right)^2 + \left(\frac{du}{ds}\right)^2 + \left(\frac{dz}{ds}\right)^2 + \left(\frac{dv}{ds}\right)^2 + \left(\frac{d\gamma}{ds}\right)^2 \\
&= \left(\frac{w - w(s_i)}{s - s_i}\right)^2 + \left(\frac{u - u(s_i)}{s - s_i}\right)^2 + \left(\frac{z - z(s_i)}{s - s_i}\right)^2 + \left(\frac{v - v(s_i)}{s - s_i}\right)^2 + \left(\frac{\gamma - \gamma(s_i)}{s - s_i}\right)^2 \\
&= \frac{(w - w(s_i))^2 + (u - u(s_i))^2 + (z - z(s_i))^2 + (v - v(s_i))^2 + (\gamma - \gamma(s_i))^2}{(s - s_i)^2}
\end{aligned}
\tag{2.6}
$$

and thus have

$$
(w - w(s_i))^2 + (u - u(s_i))^2 + (z - z(s_i))^2 + (v - v(s_i))^2 + (\gamma - \gamma(s_i))^2 - (s - s_i)^2 = 0. \tag{2.7}
$$

Thus, we have the system of equations

$$
\begin{cases}
F(\omega, \gamma) = 0 \\
(w - w(s_i))^2 + (u - u(s_i))^2 + (z - z(s_i))^2 + (v - v(s_i))^2 - (s - s_i)^2 = 0 \\
w = \frac{u - u(s_i)}{s - s_i} \\
z = \frac{v - v(s_i)}{s - s_i} \\
s - s_i = \Delta s,
\end{cases}
\tag{2.8}
$$

five equations and five unknowns. Newton's Method is used to solve this system, the solution $\left((w, v, z, v)^T, \gamma\right) = (\omega(s_{i+1}), \gamma(s_{i+1}))$.

AUTO actually uses pseudo-arclength continuation. The difference between arclength and pseudo-arclength continuation is that weights can be utilized in equation (2.7). We did not utilize this weighting, and thus for our calculations, AUTO essentially used arclength continuation.

2.2 Stability Analysis

Let $\omega(x, t) = (u(x, t), v(x, t))^T$ be an equilibrium solution of the Thomas System. If small perturbations of ω converge to ω as $t \to \infty$, then we say ω is stable and attracting. The Stability System computes solution of the Thomas System over time. One can see if a particular solution is non-attracting by viewing the solutions over time evolving away from the equilibrium solution. If the solutions over time converge to the equilibrium solution, then we can only suspect that the equilibrium is stable and attracting. We can only assume, since we do not know that for at a later time the solutions would evolve away from the equilibrium.

Figure 2.2 shows a sample run of the Stability System starting with $\gamma = 200$ and $d = 500$. In this run, the Stability System began with a perturbation of the homogeneous equilibrium and over

time solved the system. Figure 2.2 shows the solution evolution over time.
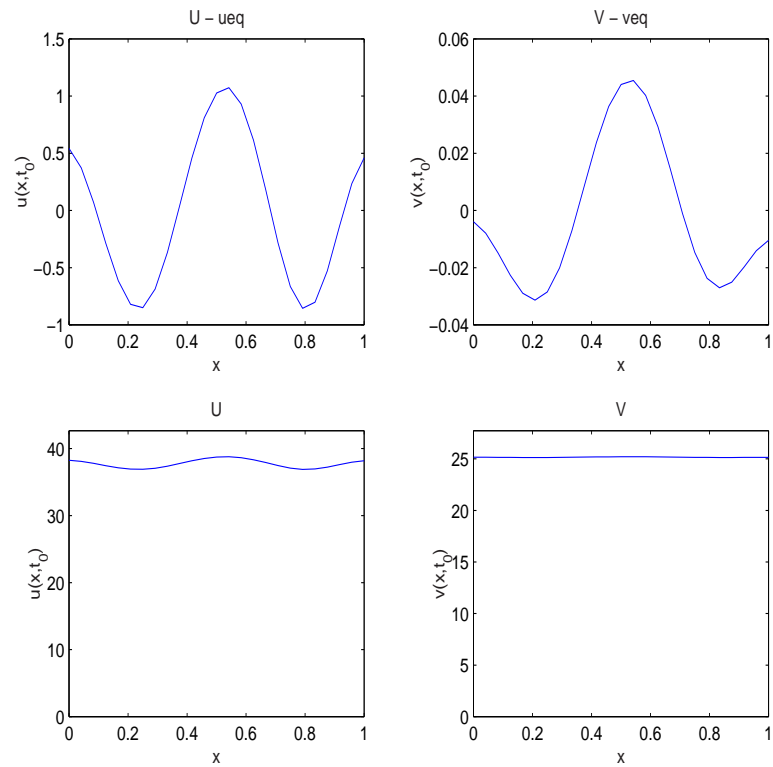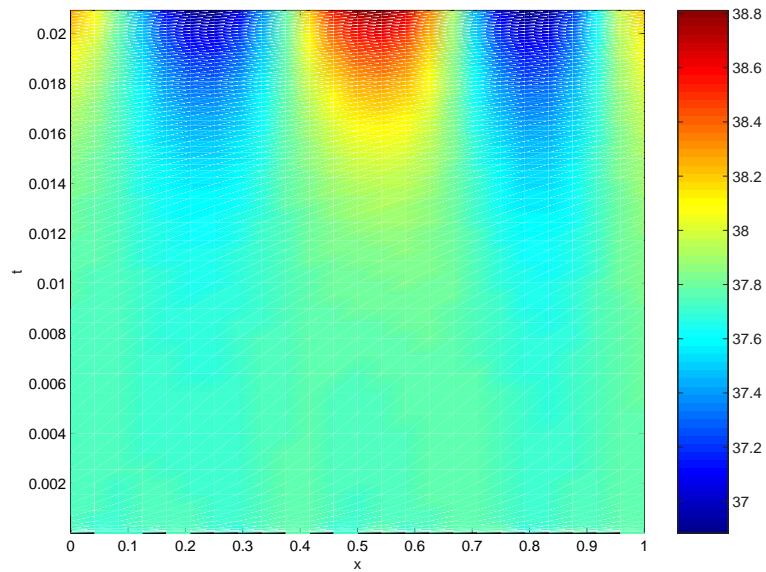
Figure 2.1: Sample run of the Stability System

Figure 2.2: Evolution of Solutions from Stability System (color indicates value of $u(x,t)$)

The Stability System is an iterative method which uses a Discrete Cosine Transform to transform the Thomas System of partial differential equations into an algebraic system. The algebraic system is then solved, and the solution is transformed back to the PDE space by the Inverse Discrete Cosine Transform. This is a standard technique in solving differential equations. Readers may recall a analogous process in ordinary differential equations with the use of the Laplace Transform.
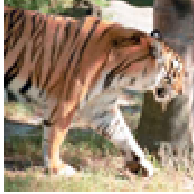
Chapter 3

Bifurcation Structure of Thomas System

Thus far, we have shown that the Thomas System has a linearly stable homogeneous equilibrium (in the absence of diffusion). Thus, it can show Turing instabilities. We now want to determine where along the homogeneous solution these instabilities occur. To determine where these instabilities occur, we will vary control parameters in the Thomas system to determine changes in the qualitative nature of the system. These qualitative changes are known as bifurcations.

3.1 Background

The simplest example of a bifurcation is the means by which fixed points are created and eliminated in a system, taken from [1]. Consider the simple system $f_a(x) = a - x^2$, a one-parameter family of functions. An alternative way of defining this system is $f(a,x) = a - x^2$, which more clearly emphasizes the dependence on the control parameter a. For our discussion, we will consider $f : I \times \mathbb{R} \to \mathbb{R}$ with $I \subset \mathbb{R}$.

Fix $a \in I$, and consider an $x \in \mathbb{R}$ such that $f_a(x) = x$. x is called a fixed point of f_a. For our particular system, the fixed points of f_a are determined by

$$f_a(x) = a - x^2 = x$$
$$-x^2 - x + a = 0$$
$$x^2 + x - a = 0$$
$$x = \frac{-1 \pm \sqrt{1 + 4a}}{2}.$$

The fixed points of our system are dependent on the control parameter a. Thus, we can see that for $a < -\frac{1}{4}$, no real fixed points exist. For $a = -\frac{1}{4}$, one fixed point exists, namely $x = -\frac{1}{2}$. Finally for $a > -\frac{1}{4}$, two real fixed points exist. Figure 3.1 shows the creation of the fixed points as a varies from -1 to 1.

The parameter value at which the number of fixed points changes is called a bifurcation value. In our system, the point $\left(-\frac{1}{4}, -\frac{1}{2}\right)$ is a bifurcation point, since one fixed point is created at $a = -\frac{1}{4}$.
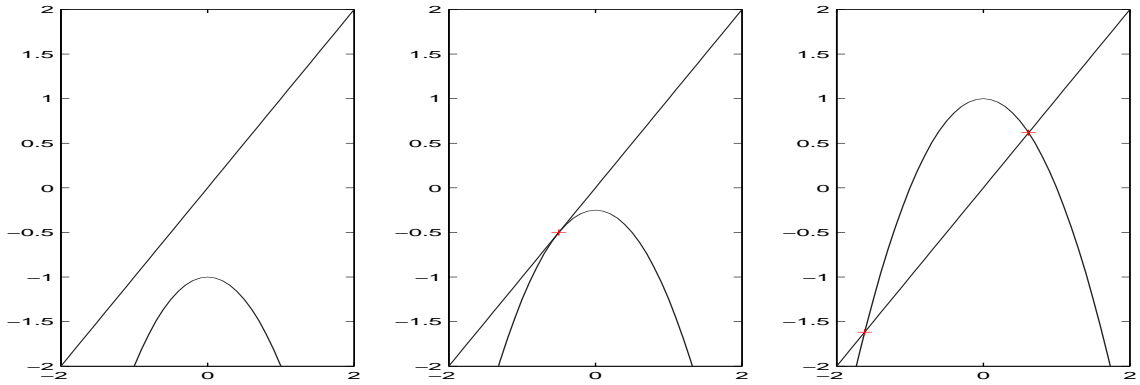
Figure 3.1: The graphs of $y = x$ and $y = a - x^2$ for $a = -1, -.25, 1$.
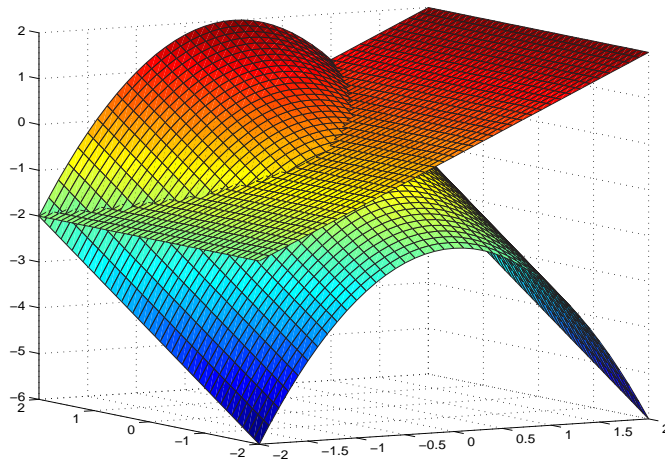

Figure 3.2: Intersection of the graphs $y = x$ and $y = a - x^2$ as a varies.

The bifurcation value $a = -\frac{1}{4}$ is a particular type of bifurcation called a tangent bifurcation. The tangent bifurcation occurs in systems of one-dimension, for which f_a' is $+1$, and thus is tangent to the line $y = x$. As a varies, the point at which two fixed points are created is called a saddle-node bifurcation. In our system, $a > -\frac{1}{4}$ is a saddle-not bifurcation.

You can clearly see how, as a is varied, the fixed points are created and changed by Figure 3.1.

The bifurcations in the previous example were based on the number of fixed points present in the system. This is not the only qualitative notion of a system for which bifurcations can occur. For the Thomas system, bifurcations will occur when the number of non-trivial equilibrium solutions change as a control parameter varies, namely γ. These bifurcations are where Turing instabilities exist, and where spatial patterns can be formed.

3.2 Analytic Determination of Bifurcations

Much of the work presented in this thesis is quantitative in nature. However, there is some information we can determine analytically. We have thus far determined that the Thomas system will exhibit Turing instabilities, as described in Chapter 1.

The first step in studying the spatial pattern formation of the Thomas system is to determine where along the homogeneous equilibrium the solution is unstable with respect to perturbations. One means by which to obtain this information is to utilize AUTO to determine where these bifurcations occur. This will, under good circumstances, determine bifurcations along the homogeneous equilibrium. We are not, however, guaranteed that AUTO will find all bifurcations along the homogeneous equilibrium. One circumstance for which AUTO may not detect a bifurcation is if the control parameter is varied at too great a rate.

It would be of great benefit to have an analytical means of determining all bifurcations along the homogeneous equilibrium. In [6], we find a standard means of analytically determining all of the bifurcations along the homogeneous equilibrium, which we will develop here. Also of interest is the inherit symmetry of the non-homogeneous solutions at the bifurcations. We will show that if you have the first bifurcation along the homogeneous equilibrium, you can very easily generate the others.

3.2.1 Derivation of Stability Changing Bifurcations

We wish to write the linearized form of the Reaction-Diffusion equation in a slightly different way, thus

$$\begin{aligned} \mathbf{w}_t &= \gamma A \mathbf{w} + D \Delta \mathbf{w} \\ &= (\gamma A - D\Delta)(\mathbf{w}). \end{aligned} \tag{3.1}$$

Since the family of eigenfunctions forms a complete basis for the set of solutions, we can substitute for the Δ operator to further transform the Reaction-Diffusion equation into

$$\begin{aligned} \mathbf{w}_t &= (\gamma A - \lambda_n D)\mathbf{w} \\ &= B_n \mathbf{w}. \end{aligned} \tag{3.2}$$

Non-trivial equilibrium solutions occur exactly when $|B_n| = 0$. The γ values for which $|B_n| = 0$ correspond to bifurcations from the homogeneous equilibrium. Thus, we need to calculate these γ values, and thus will know where the Turing instabilities occur along the homogeneous equilibrium.

We will define a function f of γ, d and $n \in \mathbb{Z}^+$, such that by fixing d, the roots of f are the loca-

tions of the bifurcations from the homogeneous equilibrium associated with the nth eigenfunction.

$$
\begin{aligned}
f(\gamma,d,n) &= \left| \gamma \begin{pmatrix} f_u & f_v \\ g_u & g_v \end{pmatrix} - (n^2\pi^2) \begin{pmatrix} 1 & 0 \\ 0 & d \end{pmatrix} \right| \\
&= \left| \begin{pmatrix} \gamma f_u - n^2\pi^2 & \gamma f_v \\ \gamma g_u & \gamma g_v - n^2\pi^2 d \end{pmatrix} \right| \\
&= \left(\gamma f_u - n^2\pi^2 \right)\left(\gamma g_v - n^2\pi^2 d \right) - \gamma^2 f_v g_u \\
&= (f_u g_v)\gamma^2 - (n^2\pi^2 d f_u)\gamma - (n^2\pi^2 g_v)\gamma - (n^2\pi^2)^2 d - (f_v g_u)\gamma^2 \\
&= (f_u g_v - f_v g_u)\gamma^2 - n^2\pi^2(d f_u + g_v)\gamma - n^4\pi^4 d.
\end{aligned}
\tag{3.3}
$$

By fixing both d and n, and utilizing Maple, we can solve for the roots of f, and thus the bifurcations from the homogeneous equilibrium. This can be an tedious task to find bifurcations. An alternative method is to exploit the symmetry of the solutions to use the initial bifurcation to calculate further bifurcations.

Let (u_0,v_0) be the equilibrium solution for γ_0 ($n=0$). Define the nth concatenation of (u_0,v_0) to be, if n is even,

$$
w(x) = \begin{cases}
u_0(nx) & , 0 \leq x < \frac{1}{n} \\
u_0(2-nx) & , \frac{1}{n} \leq x < \frac{2}{n} \\
\vdots & \\
u_0(nx-n+2) & , \frac{n-2}{n} \leq x < \frac{n-1}{n} \\
u_0(n-1-nx) & , \frac{n-1}{n} \leq x \leq 1
\end{cases}
$$

$$
z(x) = \begin{cases}
v_0(nx) & , 0 \leq x < \frac{1}{n} \\
v_0(2-nx) & , \frac{1}{n} \leq x < \frac{2}{n} \\
\vdots & \\
v_0(nx-n+2) & , \frac{n-2}{n} \leq x < \frac{n-1}{n} \\
v_0(n-1-nx) & , \frac{n-1}{n} \leq x \leq 1
\end{cases}
$$

and if n is odd,

$$w(x) = \begin{cases} u_0(nx) & , 0 \leq x < \frac{1}{n} \\ u_0(2 - nx) & , \frac{1}{n} \leq x < \frac{2}{n} \\ \vdots & \\ u_0(nx - n + 3) & , \frac{n-3}{n} \leq x < \frac{n-2}{n} \\ u_0(n - 1 - nx) & , \frac{n-2}{n} \leq x < \frac{n-1}{n} \\ u_0(nx - n + 1) & , \frac{n-1}{n} \leq x \leq 1 \end{cases}$$

$$z(x) = \begin{cases} v_0(nx) & , 0 \leq x < \frac{1}{n} \\ v_0(2 - nx) & , \frac{1}{n} \leq x < \frac{2}{n} \\ \vdots & \\ v_0(nx - n + 3) & , \frac{n-3}{n} \leq x < \frac{n-2}{n} \\ v_0(n - 1 - nx) & , \frac{n-2}{n} \leq x < \frac{n-1}{n} \\ v_0(nx - n + 1) & , \frac{n-1}{n} \leq x \leq 1 \end{cases}$$

If u_0 and v_0 satisfy homogeneous Neumann boundary conditions, then so does the nth concatenation of u_0 and v_0. If u_0 and v_0 are smooth, then the nth concatenation of u_0 and v_0 are smooth. By the Chain Rule, we can see that $\Delta w = n^2 \Delta u_0$ and $\Delta z = n^2 \Delta v_0$.

Theorem 3.1. *If (u_0, v_0) are non-trivial equilibrium solutions for γ_0 with homogeneous Neumann boundary conditions for some d, then the nth concatenation of (u_0, v_0), is a non-trivial equilibrium solution for $n^2 \gamma_0$ under homogeneous Neumann boundary conditions.*

Proof. Without loss of generality, we will prove the theorem for u_0. Let $w(x)$ be the nth concatenation of u_0. u_0 being an equilibrium solution requires for all $x \in [0, 1]$,

$$0 = \gamma_0 A u_0(x) + D \Delta u_o(x).$$

For w to be a non-trivial equilibrium for $n^2 \gamma_0$, we must show $0 = (n^2 \gamma_0) Aw + D\Delta w$. We know that $w(x) = u_0(nx + b)$ for $x \in [0, 1]$ and $0 \leq nx + b \leq 1$, since w is the nth concatenation of u_0. Thus, we have $\Delta w(x) = n^2 \Delta u_0(nx + b)$. So, we can write

$$(n^2 \gamma_0) Aw(x) + D\Delta w(x) = (n^2 \gamma_0) A u_0(nx + b) + n^2 D \Delta u_0(nx + b)$$
$$= n^2 (\gamma_0 A u_0(nx + b) + D \Delta u_0(nx + b))$$
$$= 0$$

■

3.2.2 Comparison of Bifurcations from Analysis and AUTO

The use of AUTO to generate solutions along bifurcations has its drawbacks. First, AUTO is not guaranteed to find all bifurcations.

> The general rule of thumb with AUTO is that if it finds something, it's there. But just because it doesn't find something doesn't mean it's not there.

Unfortunately, since AUTO relies on numerical computations (which have errors associated with them), this general rule can be broken, as we will see.

The previous section derives a means by which to generate a certain number of bifurcation points at which Turing instabilities will occur. This section will, for particular choices of d, compare the bifurcations calculated, and those found by AUTO. For this, we will find the first few bifurcation points for $d \in \{200, 500, 1000, 5000\}$.

In Tables 3.2.2, 3.2.2 and 3.2.2 we can see a significant difference in the values for the bifurcation points analytically determined and those computed by AUTO. We believe the error lies in those bifurcation points generated by AUTO. For all AUTO calculations done for this work, we specified a grid size of 20 in AUTO. We believe that as d increases, the numerical complexity increases, requiring a refinement of the grid. We, unfortunately, have not had time to test this theory.

Table 3.1: Some Bifurcation Points for $d = 200$

Index	Calculated	Found by AUTO
0	11.59091676	11.59093
1	46.36366704	46.36367
2	104.3182509	104.3183
3	185.4546682	185.4547
4	289.7729190	289.7727
5	417.2730033	417.2730
6	539.9670228	539.9670

Table 3.2: Some Bifurcation Points for $d = 500$

Index	Calculated	Found by AUTO
0	11.20794733	11.20795
1	44.83178933	44.83182
2	100.8715260	100.8727
3	179.3271573	179.3476
4	280.1986832	280.3793
5	403.4861038	
6	549.1894191	555.1231

Table 3.3: Some Bifurcation Points for $d = 1000$

Index	Calculated	Found by AUTO
0	11.08789331	11.08789
1	44.35157322	44.35160
2	99.79103976	99.79220
3	177.4062929	177.4256
4	277.1973326	277.3861
5	399.1641591	400.4164
6	543.3067720	
7	709.6251715	
8	898.1193577	

Table 3.4: Some Bifurcation Points for $d = 5000$

Index	Calculated	Found by AUTO
0	10.99435321	10.99435
1	43.97741284	43.97743
2	98.94917888	98.95034
3	175.9096514	175.9415
4	274.8588304	275.0295
5	395.7967157	396.8544
6	538.7233073	543.6687
7	703.6386053	714.8568
8	890.5426100	

3.3 Bifurcation Structure

Having determined the bifurcations from the homogeneous equilibrium, we will now use AUTO to determine the Bifurcation diagrams for these bifurcations. The bifurcation diagrams produced by AUTO exhibit some interesting behavior. We see potential situations where secondary bifurcations along the branch are followed, producing branches that are not symmetric with the branch of the first bifurcation point (Figure 3.3.1 is an example of this). This could be an indicator of a symmetry-breaking bifurcation.

3.3.1 Bifurcation Diagrams for $d = 200$

This is the form that we would expect, through symmetry (Thm 3.1), all bifurcation diagrams calculated for this thesis to have. We see the bifurcation diagram following a path, but ultimately returning to the initial bifurcation along the homogeneous equilibrium.
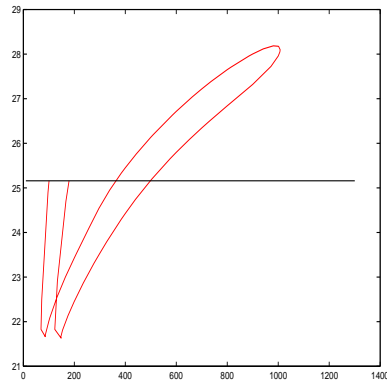
Figure 3.3: Bifurcation branch at $\gamma = 11.59093$ and $d = 200$
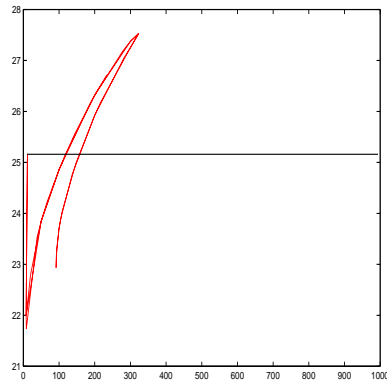
Figure 3.4: Bifurcation branch at $\gamma = 46.36367$ and $d = 200$
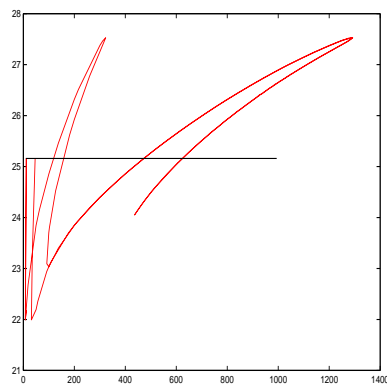
The following four diagrams illustrate situations in which errors occurred in AUTO. During this calculation, the path ultimately ended in a computational error within AUTO.
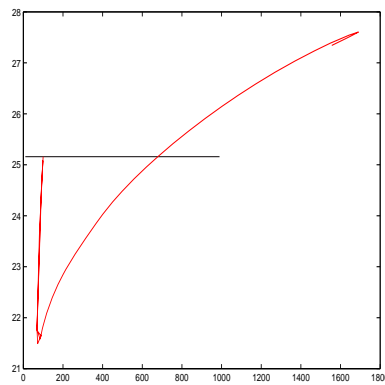
Figure 3.5: Bifurcation branch at $\gamma = 104.3183$ and $d = 200$
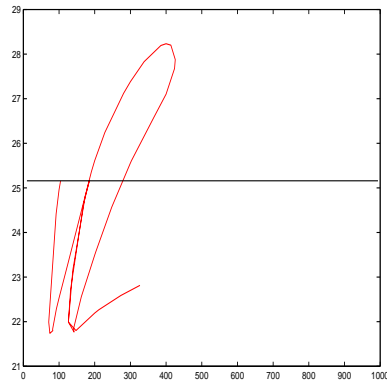

Figure 3.6: Bifurcation branch at $\gamma = 185.4547$ and $d = 200$
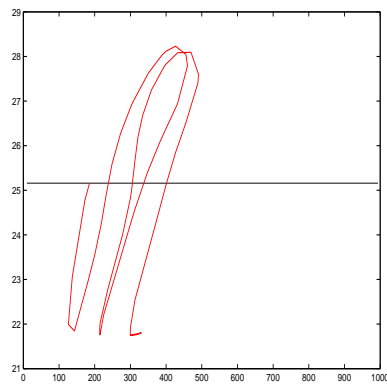
Figure 3.7: Bifurcation branch at $\gamma = 289.7737$ and $d = 200$
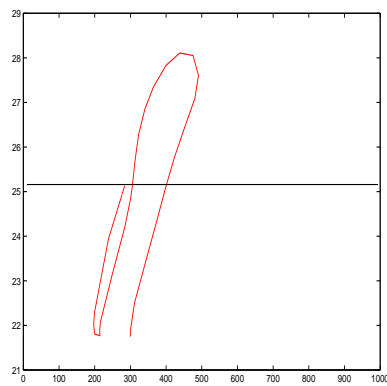
Figure 3.8: Bifurcation branch at $\gamma = 417.2730$ and $d = 200$
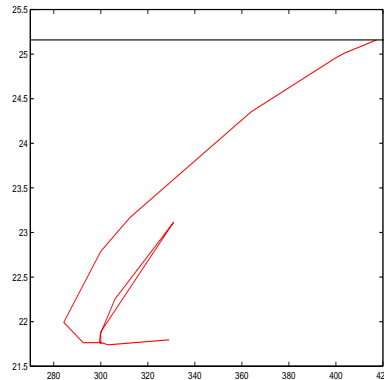
The last diagram shows an example of multiple branch jumping, potentially. The path of this branch does not even resemble the form of Figure 3.3.1. We would suspect that there are branches that are close together or even intersect.

Figure 3.9: Bifurcation branch at $\gamma = 539.9670$ and $d = 200$
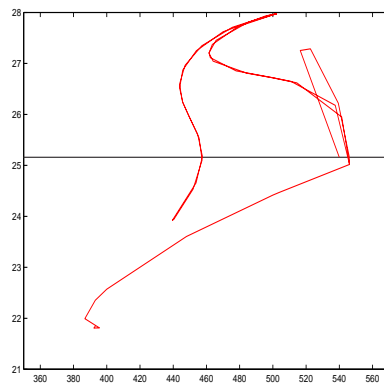
In the following three sections, we see further examples of bifurcation diagrams, with d varying.

3.3.2 Bifurcation Diagrams for $d = 500$

Figure 3.10: Bifurcation branch at $\gamma = 11.20795$ and $d = 500$
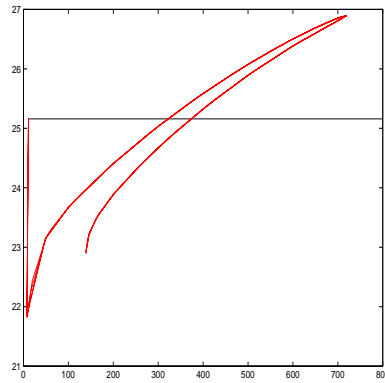
Figure 3.11: Bifurcation branch at $\gamma = 44.83182$ and $d = 500$
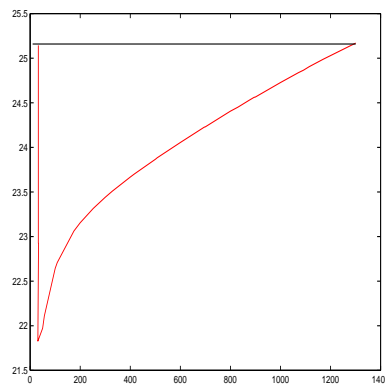
Figure 3.12: Bifurcation branch at $\gamma = 100.8727$ and $d = 500$
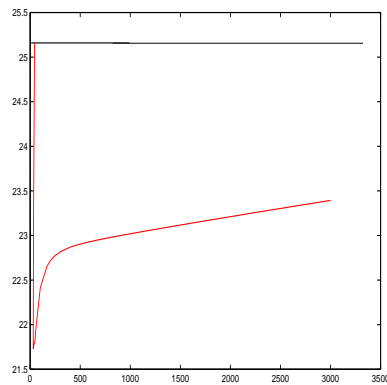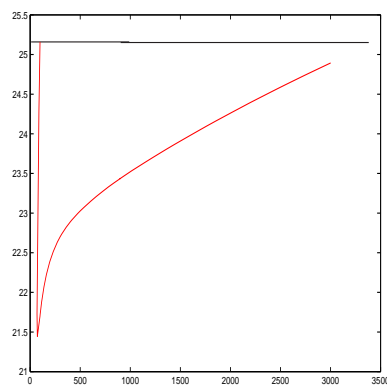
Figure 3.13: Bifurcation branch at $\gamma = 179.3476$ and $d = 500$
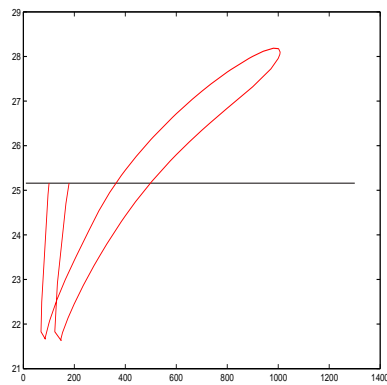
Figure 3.14: Bifurcation branch at $\gamma = 280.3793$ and $d = 500$
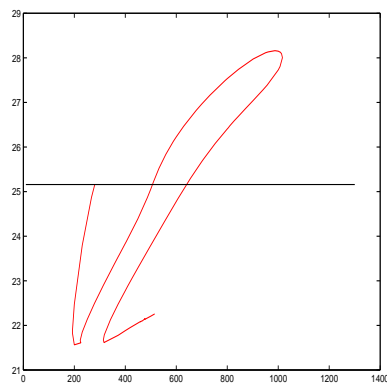
Figure 3.15: Bifurcation branch at $\gamma = 555.1231$ and $d = 500$
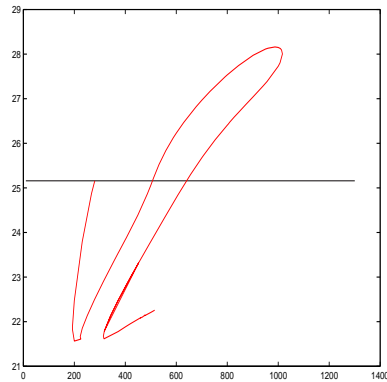

3.3.3 Bifurcation Diagrams for $d = 1000$

Figure 3.16: Bifurcation branch at $\gamma = 11.08789$ and $d = 1000$
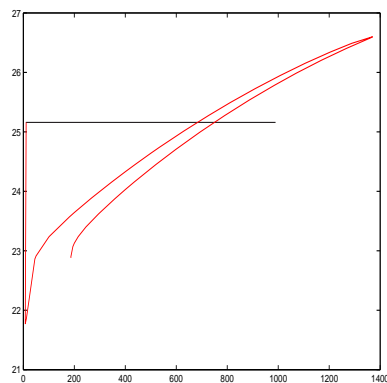
Figure 3.17: Bifurcation branch at $\gamma = 44.35160$ and $d = 1000$
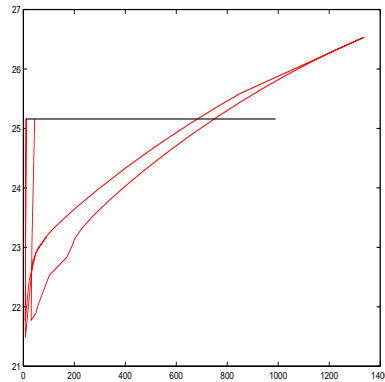
Figure 3.18: Bifurcation branch at $\gamma = 99.79220$ and $d = 1000$

Figure 3.19: Bifurcation branch at $\gamma = 277.3861$ and $d = 1000$
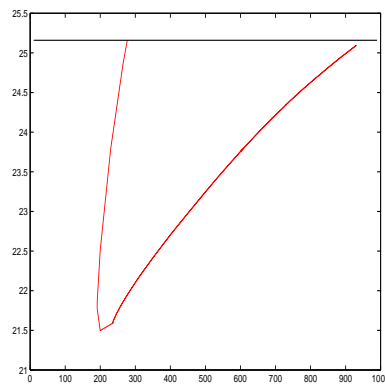
Figure 3.20: Bifurcation branch at $\gamma = 277.3861$ and $d = 1000$
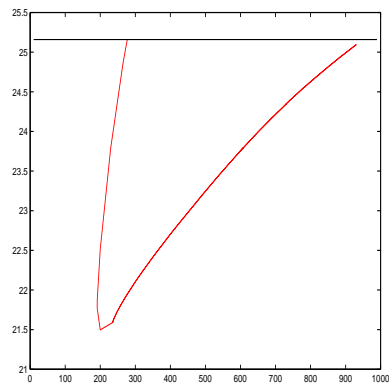
3.3.4 Bifurcation Diagrams for $d = 5000$

Figure 3.21: Bifurcation branch at $\gamma = 10.99435$ and $d = 5000$
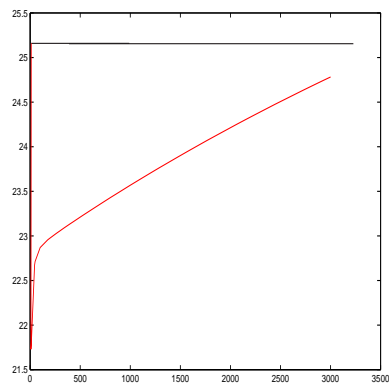
Figure 3.22: Bifurcation branch at $\gamma = 43.97743$ and $d = 5000$

Figure 3.23: Bifurcation branch at $\gamma = 98.95034$ and $d = 5000$

Figure 3.24: Bifurcation branch at $\gamma = 175.9415$ and $d = 5000$
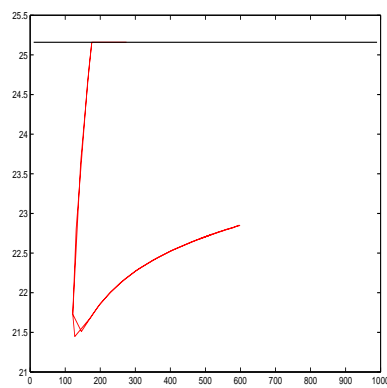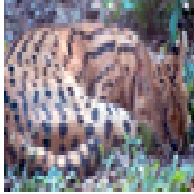
# Chapter 4

Stability of Thomas System

Thus far we have been concerned with the instability of the homogeneous solution, and thus where patterns will form. Now, we will shift out focus to the actual solutions along these bifurcations. Pattern formation is believed to be due to patterns of concentrations of morphogens []. Stable attracting solutions to the Thomas system will provide the patterns of concentrations of morphogens which will result in animal coat patterns.

Murray [9] provides a visual of regions of stable solutions, and what the solutions look like, in (γ, d) space. We will not only attempt to find stable solutions using AUTO and the Stability system, but we will compare these solutions to the solution space Murray provides. Murray provides no explanation in [9] as to how these stable solutions were verified. Thus, verification of this information is important.

4.1 Murray Proposed Stable Solution Space

Murray, in [9], provides the following two-dimensional picture of the regions in which various stable solutions are found for the Thomas system

Figure 4.1: Investigated regions of stable solutions in (γ, d) space.
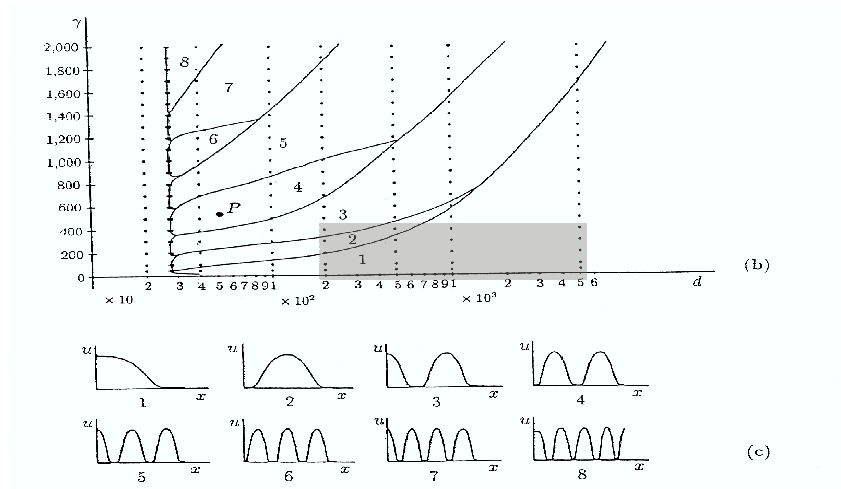
As you can see, for $\gamma = 200$ and $d = 400$, we would expect to see a stable solution like that labelled 3. We will restrict our attention to a portion of this graph for verification, as shown below.

Table 4.1 summarizes the expected stability published by Murray. We will update this table with our numerical findings in an attempt to verify these stable solutions.

Table 4.1: Published Stable Solution Forms

d	γ	Form of Stable Solution(Murray)
200	100	1
	200	2
	300	2
	400	3
500	50	1
	100	1
	200	1
	300	1
	400	2
1000	50	1
	100	1
	200	1
	300	1
	400	1
5000	50	1
	100	1
	200	1
	300	1
	400	1

4.2   Computed Stable solution space

To determine the stability of solutions at a particular γ value, we will utilize both AUTO and the Stability Software. First, solutions are found by AUTO for particular d along many bifurcation paths. Then, these solutions are imported into the Stability Software. Once imported, the solutions will be spatially perturbed and inspected to see if they "converge" to their original solution, or possibly some other solution.

What is important to note is that just because a perturbed solution, denoted w converges to itself or another solution, denoted w_c, does not necessarily mean that w_c is an attractive stable solution. The most we can say is that it seems to be an attractive stable solution. Further work would need to be done to determine through other means if w_c is an attracting stable solution.

Since we are attempting to verify results from Murray, we shall choose d to align with the results in Figure 4.1. Thus we shall have AUTO determine solutions for the following set of (γ, d)

values, namely $G \times D$, where $G = \{50, 100, 200, 300, 400\}$ and $D = \{200, 500, 1000, 5000\}$.

A convention that will be followed in the following sections is to show apparently attractive stable solutions in blue and unstable solutions in red.
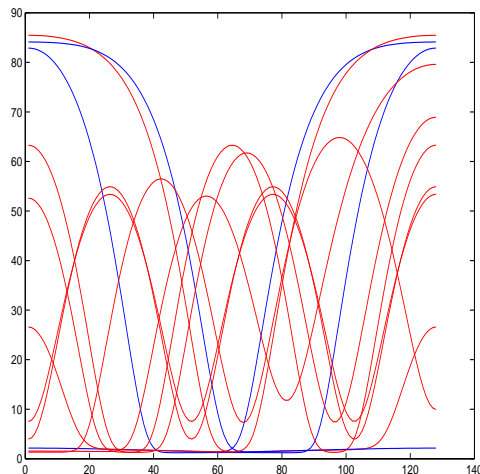
4.2.1 Apparent Stability at $(\gamma, d) = (100, 200)$

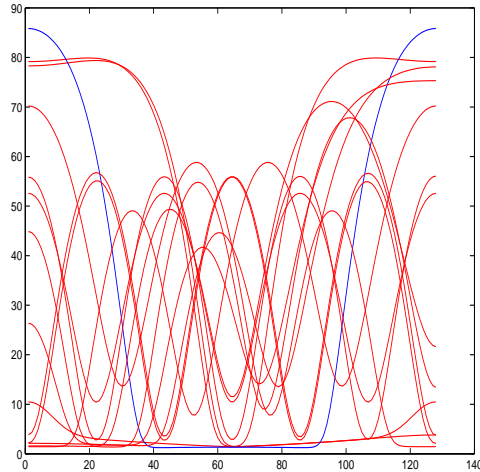Figure 4.2: Stable and Unstable solutions at $(\gamma, d) = (100, 200)$
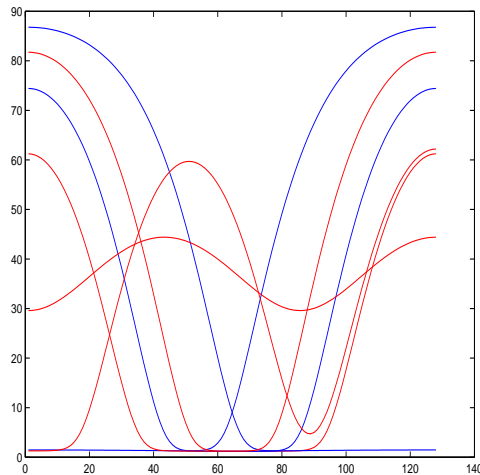
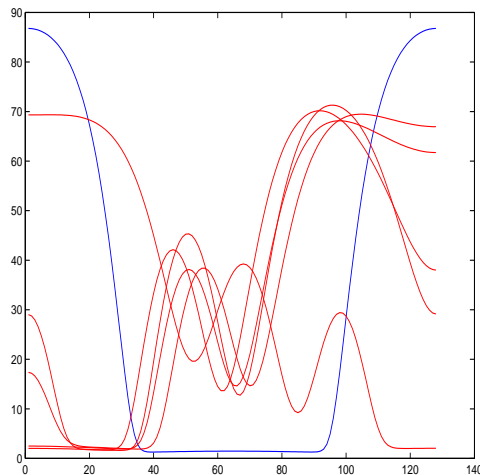
4.2.2 Apparent Stability at $(\gamma, d) = (200, 200)$

Figure 4.3: Stable and Unstable solutions at $(\gamma, d) = (200, 200)$

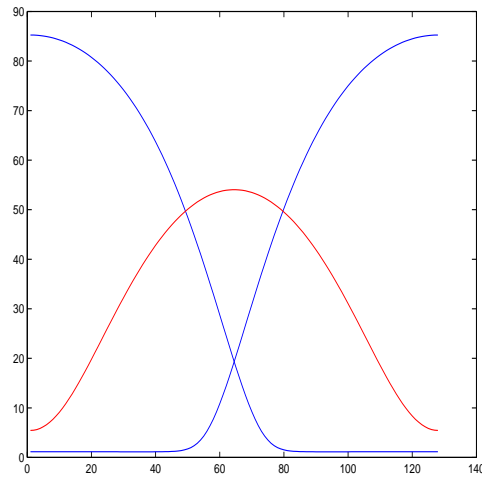### 4.2.3 Apparent Stability at $(\gamma, d) = (300, 200)$

Figure 4.4: Stable and Unstable solutions at $(\gamma, d) = (300, 200)$

4.2.4 Apparent Stability at $(\gamma, d) = (400, 200)$

Figure 4.5: Stable and Unstable solutions at $(\gamma, d) = (400, 200)$
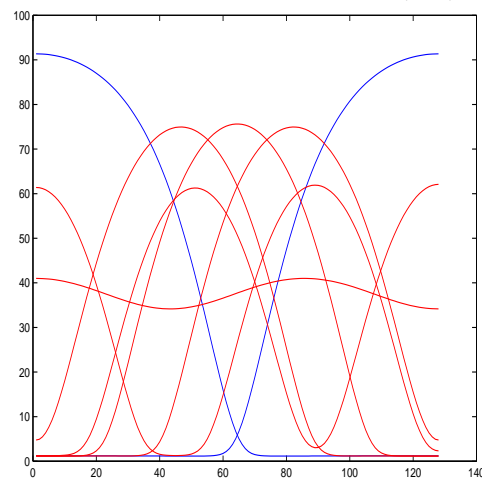

4.2.5 Apparent Stability at $(\gamma, d) = (50, 500)$

There are three solutions found for $(\gamma, d) = (50, 500)$, two from the first branch and one from the second branch. The solutions are shown in Figure 4.6. However, only two are stable.
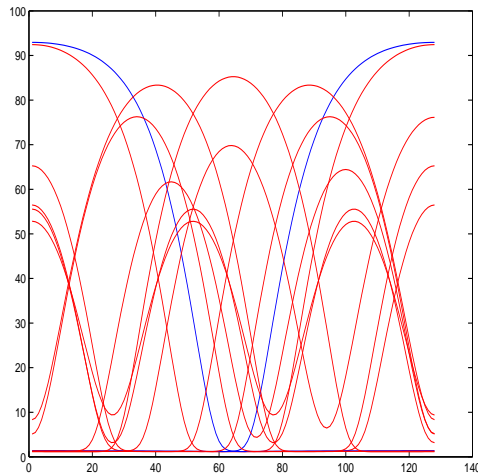
Figure 4.6: Stable and Unstable solutions at $(\gamma, d) = (50, 500)$

This adds a stable solution to the picture that Murray did not include, namely the symmetric solution of solution 1 from Figure 4.1.
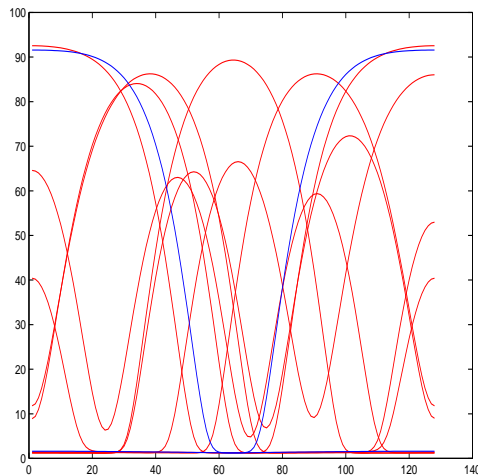
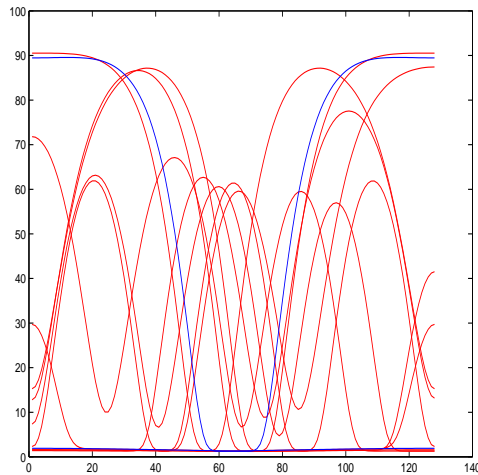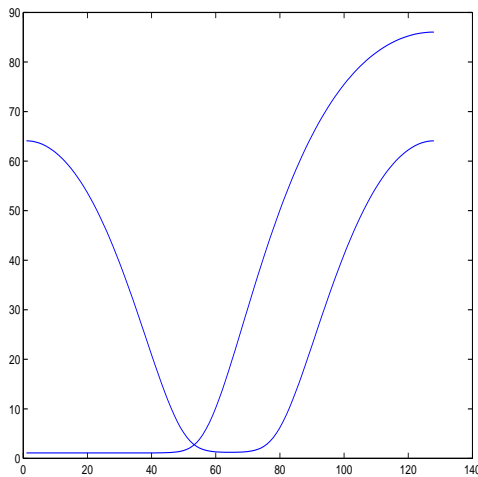### 4.2.6   Apparent Stability at $(\gamma, d) = (100, 500)$

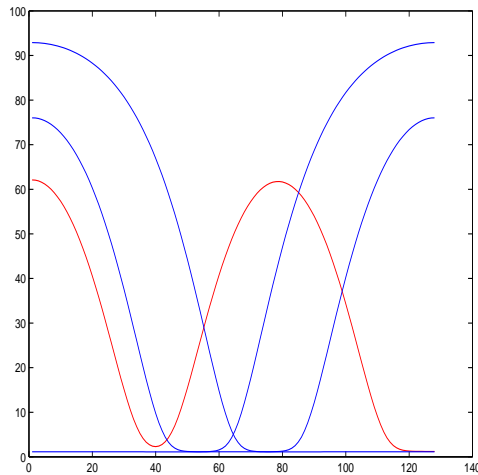Figure 4.7: Stable and Unstable solutions at $(\gamma, d) = (100, 500)$

4.2.7 Apparent Stability at $(\gamma, d) = (200, 500)$

Figure 4.8: Stable and Unstable solutions at $(\gamma, d) = (200, 500)$

4.2.8 Apparent Stability at $(\gamma, d) = (300, 500)$

Figure 4.9: Stable and Unstable solutions at $(\gamma, d) = (300, 500)$

4.2.9 Apparent Stability at $(\gamma, d) = (400, 500)$

Figure 4.10: Stable and Unstable solutions at $(\gamma, d) = (400, 500)$

4.2.10 Apparent Stability at $(\gamma, d) = (50, 1000)$

Figure 4.11: Stable and Unstable solutions at $(\gamma, d) = (50, 1000)$

4.2.11 Apparent Stability at $(\gamma, d) = (100, 1000)$

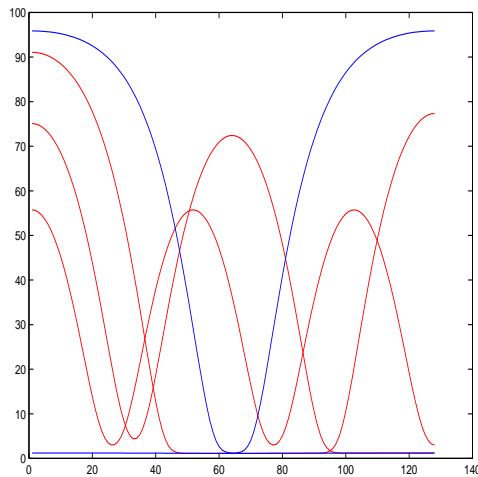Figure 4.12: Stable and Unstable solutions at $(\gamma, d) = (100, 1000)$

4.2.12 Apparent Stability at $(\gamma, d) = (200, 1000)$
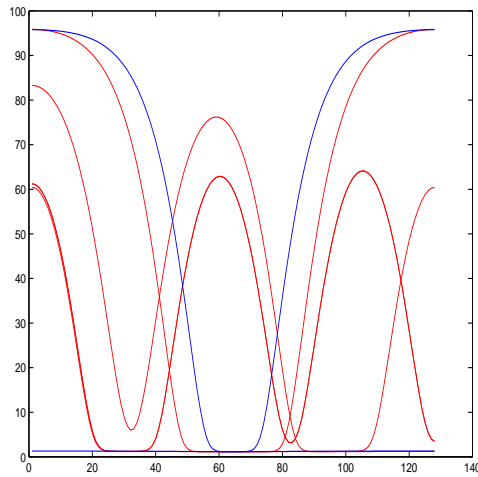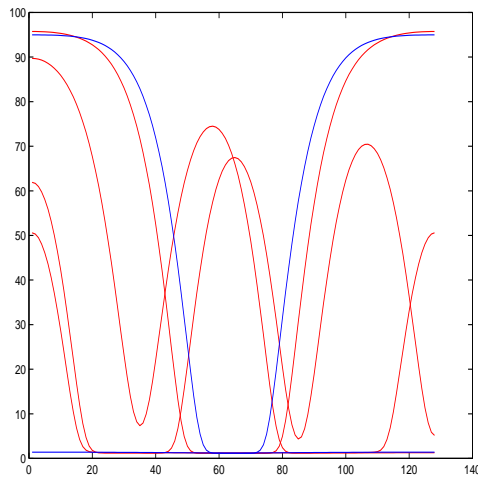
Figure 4.13: Stable and Unstable solutions at $(\gamma, d) = (200, 1000)$

4.2.13   **Apparent Stability at** $(\gamma, d) = (300, 1000)$

Figure 4.14: Stable and Unstable solutions at $(\gamma, d) = (300, 1000)$

4.2.14   **Apparent Stability at** $(\gamma, d) = (400, 1000)$

Figure 4.15: Stable and Unstable solutions at $(\gamma, d) = (400, 1000)$

4.2.15   Apparent Stability at $(\gamma, d) = (50, 5000)$

Figure 4.16: Stable and Unstable solutions at $(\gamma, d) = (50, 5000)$

4.2.16   Apparent Stability at $(\gamma, d) = (100, 5000)$

Figure 4.17: Stable and Unstable solutions at $(\gamma, d) = (100, 5000)$

4.2.17 Apparent Stability at $(\gamma, d) = (200, 5000)$

Figure 4.18: Stable and Unstable solutions at $(\gamma, d) = (200, 5000)$
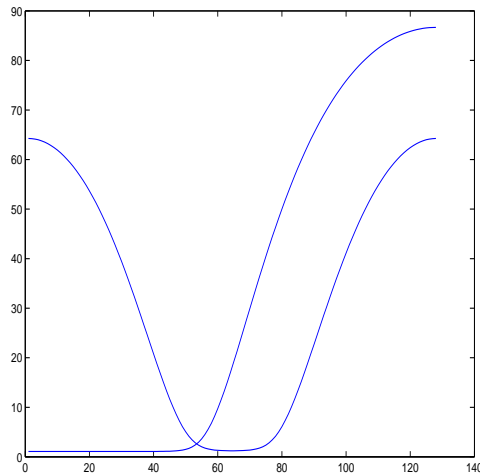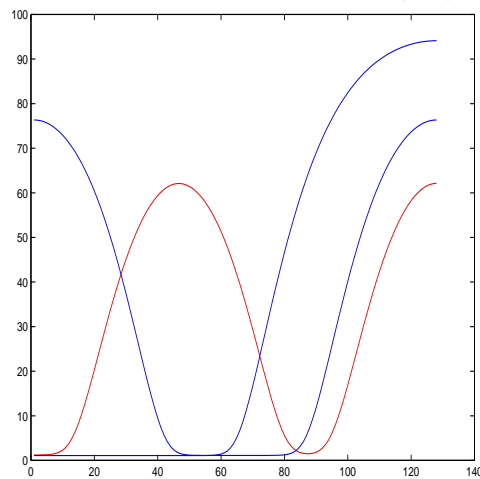

4.2.18 Apparent Stability at $(\gamma, d) = (300, 5000)$
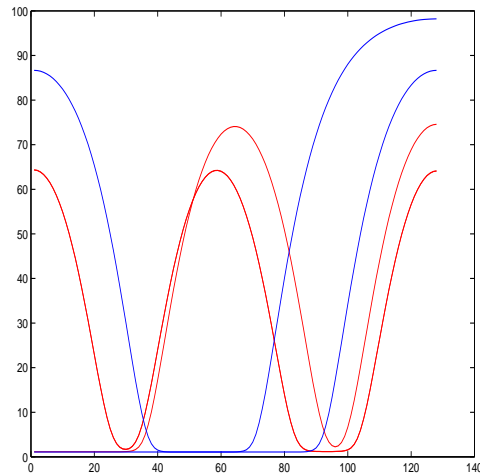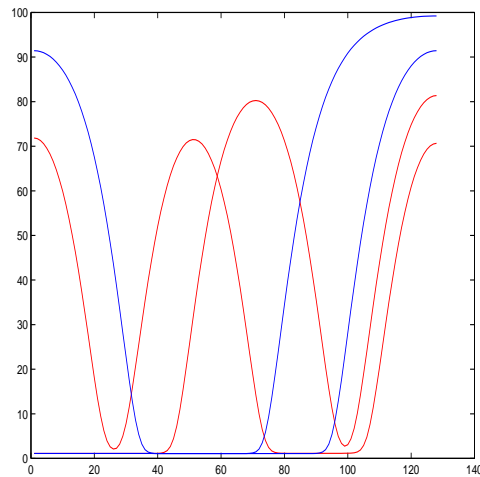
Figure 4.19: Stable and Unstable solutions at $(\gamma, d) = (300, 5000)$

4.2.19 Apparent Stability at $(\gamma, d) = (400, 5000)$

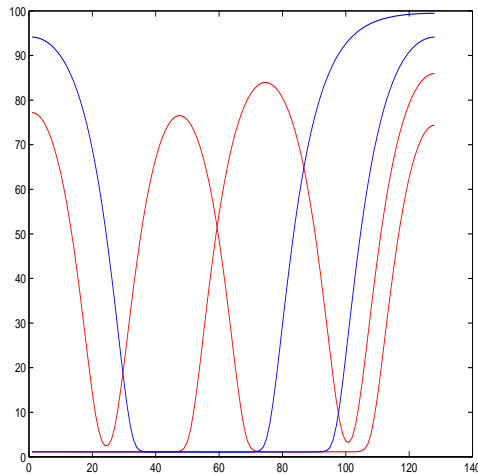Figure 4.20: Stable and Unstable solutions at $(\gamma, d) = (400, 5000)$

4.3 Comparison with Published Data

The published data from Murray [9] is not inaccurate, but not likely altogether complete. Table 4.3 provides a comparison of the forms of stable solutions published by Murray and those calculated via AUTO and the Stability System.

Table 4.2: Comparison of Stable Solution Forms

d	γ	**Form of Stable Solution(Murray)**	**Form of Stable Solution(Calculated)**
200	100	1	1, symmetric 1, symmetric 2
	200	2	1, symmetric 1, symmetric 2
	300	2	symmetric 2
	400	3	symmetric 2
500	50	1	1, symmetric 1
	100	1	1, symmetric 1
	200	1	1, symmetric 1
	300	1	1, symmetric 1
	400	2	1, symmetric 1
1000	50	1	symmetric 1, symmetric 2
	100	1	1, symmetric 1, symmetric 2
	200	1	1, symmetric 1
	300	1	1, symmetric 1
	400	1	1, symmetric 1
5000	50	1	symmetric 1, symmetric 2
	100	1	symmetric 1, symmetric 2
	200	1	symmetric 1, symmetric 2
	300	1	symmetric 1, symmteric 2
	400	1	symmetric 1, symmetric 2

What we see in this table is that there exists more stable equilibrium solutions than Murray indicated. We find that the symmetric image of the solutions from Murray are also stable. And in a few instances, we see the potential for the co-existence of solutions of different forms. This is much different than that suggested by Murray, whose data indicates only one form of solutions is stable at one time. It is important to note that the numerical errors encountered in the previous chapter when computing the bifurcation points may also affect the results for the stable solutions. Thus it is important to rerun these simulations when these numerical issues are dealt with.

Chapter 5

Conclusion

5.1 Findings

The stable solutions that Murray published in [9] may not be the entire picture. It appears that some more stable solutions exist for particular (γ, d) values for the Thomas System. However, the work in this thesis can not say definitively that this is the case; these solutions appear stable.

5.2 Further Work

There are clear areas where further research is needed. First, further development of the bifurcation structure and solutions is needed. The work in this thesis has developed only a small subset of the data to verify. Secondly, in this, numerical subtleties need to be worked out with AUTO in order to ensure convergence when following certain bifurcation branches.

A second area, and arguably most important, is the determination of the stability of the solutions generated by AUTO. The method used in this thesis provides a differing view of stable solutions than that of Murray [9]. While Murray utilized Time-Evolution to determine stability, we went one step further and utilized AUTO to compute equilibrium solutions. These solutions were then evolved over time to determine stability. Other methods, such as index calculation, should be employed in order to actually determine the stability of the solutions. This work will add more evidence to either confirm or refute the published data provided by Murray.

Chapter 6

Source Code

Listing 6.1: AUTO Thomas System

```c
#include "auto_f2c.h"
#include <math.h>

int func (integer ndim, const doublereal *u, const integer *icp,
          const doublereal *par, integer ijac,
          doublereal *f, doublereal *dfdu, doublereal *dfdp) {
    doublereal my_f, my_g, my_h, my_u, my_v;

    my_h = (13.0*u[0]*u[2]) / (1.0 + u[0] + (0.05*u[0]*u[0]));
    my_f = 150.0 - u[0] - my_h;
    my_g = 1.5*(100.0 - u[2]) - my_h;

    /**
     ** f[0] = w
     ** f[1] = -gamma*f
     ** f[2] = z
     ** f[3] = (-gamma*g) / d
     **/
    f[0] = u[1];
    f[1] = - par[0] * my_f;
    f[2] = u[3];
    f[3] = (- par[0] * my_g) / par[1];

    return 0;
```

```
}

int stpnt (integer ndim, doublereal t,
           doublereal *u, doublereal *par) {
    /**
     ** par[0] = gamma
     ** par[1] = d
     **/
    par[0] = 10.0;
    par[1] = 200.0;

    /**
     ** u[0] = u
     ** u[1] = w
     ** u[2] = v
     ** u[3] = z
     **/
    u[0] = 37.73821;
    u[1] = 0.0;
    u[2] = 25.15881;
    u[3] = 0.0;

    return 0;
}

int bcnd (integer ndim, const doublereal *par, const integer *icp,
          integer nbc, const doublereal *u0, const doublereal *u1,
          integer ijac, doublereal *fb, doublereal *dbc) {

    /** Homogenious Neumann Boundary Conditions **/
    fb[0] = u0[1];
    fb[1] = u1[1];
    fb[2] = u0[3];
    fb[3] = u1[3];

    return 0;
}
```

```c
int icnd ( integer ndim , const doublereal *par , const integer *icp ,
           integer nint , const doublereal *u , const doublereal *uold ,
           const doublereal *udot , const doublereal *upold , integer ijac ,
           doublereal *fi , doublereal *dint ) {
    return 0;
}


int fopt ( integer ndim , const doublereal *u , const integer *icp ,
           const doublereal *par , integer ijac ,
           doublereal *fs , doublereal *dfdu , doublereal *dfdp ) {
    return 0;
}


int pvls ( integer ndim , const doublereal *u ,
           doublereal *par ) {
    return 0;
}
```

Listing 6.2: AUTO Constants File

4 4 0 1	NDIM, IPS , IRS , ILP
1 0	NICP , (ICP (I) , I = 2 NICP)
20 4 3 2 1 3 4 0	NTST , NCOL , IAD , ISP , ISW , IPLT , NBC , NINT
1000 3.0 1300.0 0.0 500.0	NMX, RL0 , RL1 , A0 , A1
100 10 2 8 5 3 0	NPR , MXBF, IID , ITMX , ITNW , NWTN, JAC
1e−06 1e−06 0.0001	EPSL , EPSU , EPSS
0.001 0.0001 1.0 1	DS , DSMIN , DSMAX , IADS
0	NTHL , (/ , I , THL (I)) , I = 1 ,NTHL)
0	NTHU , (/ , I , THU (I)) , I = 1 ,NTHU)
0	NUZR , (/ , I , PAR (I)) , I = 1 ,NUZR)

Bibliography

[1] Kathleen T. Alligood, Tim D. Sauer, and James A. Yorke. *Chaos: An Introduction to Dynamical Systems*. Springer-Verlag, 1996.

[2] William E. Boyce and Richard C. DiPrima. *Elementary Differential Equations*. John Wiley & Sons, Inc., 7th edition, 2003.

[3] James Ward Brown and Ruel V. Churchill. *Fourier Series and Boundary Value Problems*. McGraw Hill, 6th edition, 2001.

[4] Jennifer Deering. Computation of the bifurcation structure of the Cahn-Hilliard equation. Master's thesis, University of Maryland, Baltimore, MD 21250, May 2002.

[5] Eusebius J. Doedel, Randy C. Paffenroth, Alan R. Champneys, Thomas F. Fairgrieve, Yuri A. Juznetsov, Bart E. Oldeman, Björn Sandstede, and Xianjun Wang. *AUTO 2000: Continuation and Bifurcation Software for Ordinary Differential Equations*. 2002.

[6] Peter Grindrod. *The Theory and Application of Reaction-Diffusion Equations: Patterns and Waves*. Clarendon Press, Oxford, 1996.

[7] John H. Mathews and Kurtis D. Fink. *Numerical Methods Using Matlab*. Prentice Hall, 1998.

[8] James D. Murray. How the leopard gets its spots. *Scientific American*, 258(3):80–87, 1988.

[9] James D. Murray. *Mathematical Biology*. Springer-Verlag, 2nd corrected edition, 1993.

[10] Lawrence Perko. *Differential Equations and Dynamical Systems*. Springer-Verlag, 3rd edition, 2000.

[11] Michael Renardy and Robert C. Rogers. *An Introduction to Partial Differential Equations*. Springer-Verlag, 1992.

[12] Evelyn Sander and Thomas Wanner. Pattern formation in a nonlinear model for animal coats. *Journal of Differential Equations*, 191:143–174, 2003.

[13] Alan M. Turing. The chemical basis of morphogenesis. *Philosophical Transactions of the Royal Society*, 237:37–72, 1952.